Peer-reviewed version available at *Molecules* **2019**, *24*, 1196; doi:10.3390/molecules24071196

Article

A Complete Assessment of Dopamine Receptor-Ligand Interactions through Computational Methods

Beatriz Bueschbell [1], Carlos A. V. Barreto [2], António J. Preto [2], Anke C. Schiedel [1] and Irina S. Moreira [2,3,*]

1 PharmaCenter Bonn, Pharmaceutical Institute, Pharmaceutical Chemistry I, University of Bonn, D-53121 Bonn, Germany; bueschbell@uni-bonn.de; schiedel@uni-bonn.de

2 Center for Neuroscience and Cell Biology, UC- Biotech Parque Tecnológico de Cantanhede, Núcleo 04, Lote B, 3060-197 Cantanhede, Portugal; cbarreto@cnc.uc.pt; martinsgomes.jose@gmail.com; Irina.moreira@cnc.uc.pt

3 Institute for Interdisciplinary Research, University of Coimbra

*Correspondence: irina.moreira@cnc.uc.pt; Tel.: +351 231 249 730

Abstract

Background: Selectively targeting dopamine receptors has been a persistent challenge in the last years for the development of new treatments to combat the large variety of diseases evolving these receptors. Although, several drugs have been successfully brought to market, the subtype-specific binding mode on a molecular basis has not been fully elucidated.

Methods: Homology modeling and molecular dynamics were applied to construct robust conformational models of all dopamine receptor subtypes (D_1-like and D_2-like receptors). Fifteen structurally diverse ligands were docked to these models. Contacts at the binding pocket were fully described in order to reveal new structural findings responsible for DR sub-type specificity.

Results: We showed that the number of conformations for a receptor:ligand complex was associated to unspecific interactions > 2.5 Å and hydrophobic contacts, while the decoys binding energy was influenced by specific electrostatic interactions. Known residues such as 3.32Asp, the serine microdomain and the aromatic microdomain were found interacting in a variety of modes (HB, SB, π-stacking). Purposed TM2-TM3-TM7 microdomain was found to form a hydrophobic network involving Orthosteric Binding Pocket (OBP) and Secondary Binding Pocket (SBP). T-stacking interactions revealed as especially relevant for some large ligands such as apomorphine, risperidone or aripiprazole.

Conclusions: This *in silico* approach was successful in showing known receptor-ligand interactions as well as in determining unique combinations of interactions, key for the design of more specific ligands.

Keywords: Dopamine receptors, Molecular Docking, Molecular Dynamics, Receptor-Ligand Interactions

Peer-reviewed version available at *Molecules* **2019**, *24*, 1196; doi:10.3390/molecules24071196

1. Introduction

Dopamine Receptors

The dopaminergic system has been intensively studied over the past 50 years due to the (patho)physiological role in modulating cognitive and motor behaviour [1,2]. Moreover, various severe neuropsychiatric and neurodegenerative disorders such as Tourette's Syndrome, schizophrenia, Parkinson's disease and Huntington's disease are believed to occur as a result of imbalances and alterations in dopamine signalling [3–5]. Dopaminergic effects are mediated by five distinct receptors ($D_{1\text{-}5}$ receptor), grouped in two classes, D_1-like and D_2-like receptors, that differ in their physiological effects and signal transduction. The D_1-like receptors, D_1 and D_5 receptors, are principally coupled to G_s proteins and enhance the activity of adenylyl cyclase, whereas D_2-like receptors, $D_{2\text{-}4}$ receptors, are primarily coupled to inhibitory G_i proteins and suppress the adenylyl cyclases' activity [1,6]. The Dopamine Receptors (DR) belong to the G-protein-coupled receptors (GPCRs), the largest and most diverse protein family in humans with approximately 800 members [7,8], and a significant target of pharmacotherapeutics. Numerous therapeutics are available on the market, foremost for the D_2R subtype [6] such as haloperidole, chlorpromazine [9], risperidone, clozapine, ziprasidone or quetiapine [10]. However, most of the commonly utilized drugs show significant side effects and nonselective profiles [10,11]. The search for a DR subtype selective therapeutics is an ongoing field of research. For example, it has been proposed that substituted 4-phenylpiperazine compounds dissect between D_3R and D_2R selectivity [12,13]. In addition, the aminotetraline derivative 7-OH-DPAT was identified as selective D_3R agonist [14,15], whereas it was shown that most D_4R available therapeutics are not selective [13], with only one exception, haloperidole [16]. Sampson *et al.* synthesized selective D_4R ligands with K*i* values in the lower nanomolar range, based on the piperazine analogue of haloperidole as pharmacophore to target erectile dysfunction [16]. This piperazine moiety of haloperidole was further explored in other studies, leading to the development of aripiprazole, a next-generation atypical antipsychotic, which is highly selective for D_2R and D_2R/D_3R heterodimers, displaying properties of D_2R agonist and antagonist [17]. For D_1-like receptors, D_1R and D_5R, the achievement of subtype selective ligands has been even more challenging [18,19]. SKF83959 was the only selective agonist attained for the D_1R so far, while D_5R completely lacks a selective ligand [20,21]. SCH23390 has been proposed to be the only D_1-like DR selective antagonist [22].

In summary, finding new highly selective ligands for all DR subtypes, especially for the D_1-like subtypes, which are poorly described would be a major step forward in the field [23].

Computer Aided Drug Design

The strive for finding new and effective therapeutics led to a growing interest in the use of Computer Aided Drug Design (CADD). Originally developed for High-Throughput Screening (HTS) of compound libraries, the use of CADD nowadays plays an important role in drug discovery [24]. Modeling three-dimensional (3D) target proteins help to visualize, analyse and optimize known ligands and discover new lead compounds [25]. The CADD pipeline can be classified in two general categories: structure-based and ligand-based, dependent on the available information about the topic of investigation [25]. A structure-based CADD is used when the target, e.g. a receptor, is known and so compound libraries can be screened to find suitable structures for the target. Usually protein-ligand docking studies are performed or ligands are designed *de novo* and are then used for compound library screening to test possible lead structures experimentally. *Vice-versa*, a ligand-based CAAD procedure is used when ligand structure information is provided to create pharmacophore models and to perform virtual screening [24]. All in all, CADD faces the challenges of identifying novel targets and their ligands, for example to treat common and rare diseases [26].

Aim

Modeling G protein-coupled receptors (GPCRs) remains challenging due to the complex structure of these membrane proteins and the lack of structural information about the desired receptor to target, however CADD methods have undoubtedly shed light on the subject. The recent boom on X-ray crystallography structures resolved, leads to a more promising application of CADD. In this work, we used tools of structure-based CADD to investigate the receptor-ligand properties of all DR-subtypes with marketed DR therapeutics. In particular, we applied i) homology modeling by using the resolved X-ray crystallography structures of the dopamine receptors D_2, D_3R and D_4R [27–29], ii) performed Molecular Dynamics (MD) of the 5 model structures, and iii) molecular docking studies of 15 ligands targeting different conformational rearrangements' of DR subtypes. The binding energies, number of conformations as well as the distances between ligands and receptor interacting residues of the binding pocket were calculated for all complexes. The interaction between ligands and receptors were analysed using an in-house pipeline that takes advantage of BINding ANAlyzer (BINANA), a python implemented algorithm for analysing ligand binding [30]. The main goal was to reveal new structural findings to help explain DR sub-type specificity.

2. Results

2.1. Homology modelling of Dopamine Receptors

The homology models were generated using MODELLER (version modeler 9.19, released Jul 25th, 2017) [31] and the resolved crystal structures of the D_2R (PDBid: 6CM4) [29], D_3R (PDBid: 3PBL) [32] and D_4R (PDBid: 5WIU) [28] retrieved from the Protein Data Bank (PDB) [33]. The most suitable template to each DR was selected according to the percentage of similarity obtained upon sequence alignment by BLAST [34] in combination with ClustalOmega [35]. The D_1R was modelled with the D_3R crystal structure (PDBid: 3PBL [32]; 35.0 % identity with BLAST and 39.5 % with ClustalOmega). The D_2R model was modelled with the crystallographic structure of the D_2R complexed with risperidone (PDBid: 6CM4) [29], (total similarity 97.0% with BLAST and 100.0 % with ClustalOmega). The D_3R was modelled using 3PBL as template with a total sequence similarity of 93.0 % by BLAST and 99.3 % with ClustalOmega. Similar scores were obtained for the D_4R and the 5WIU template 93.0 % (BLAST)/ 100.0 % (ClustalOmega). Lastly the D_5R model was calculated using the D_4R (PDBid: 5WIU [28]) template as it displayed a total similarity of 35.0 % (BLAST)/ 39.1 % (ClustalOmega). We also calculated the similarity of the TMs in relation to the respective template and the results are summarized in **Table S1**. All TMs of the D_2-like subtypes showed almost 100 % identity with their crystal structure templates, which is also in line with the total similarity. Regarding the D1-like subtypes, the receptors were not modelled with their own crystal structure template since they are not available yet. D_1R was modelled with the crystal structure of the D_3R (PDBid: 3PBL) whereas D_5R was modelled with the crystal structure of the D_4R (PDBid: 5WIU). For the D_1R an average TM similarity with its template was 41.0 %, compared to a total similarity of 39.5 %, while for the D_5R 36.0 % TM identity was calculated compared to the total similarity of 39.1 %. Hence, also for the D_1-like subtypes no differences between the TM similarity and the total similarity with their template were obtained. Furthermore, for the D_1R the highest similarity between the model and its template was observed for TM1-3, whereas for D_5R was TM2, TM3 and TM7. Consequently, the TM2 and TM3 seem to be conserved among all DR subtypes. In summary, the results indicate that the TM definition used for calculating the DR models did not affect the model identity towards its template.

Different metrics and scores were used to choose the most accurate models provided by MODELLER in order to perform MD and molecular docking. DOPE (Discrete Optimized Protein Energy) [36] scores are MODELLER's standard metrics and were utilized in combination with visual inspection to remove models which were not calculated correctly. DOPE is specific for a given target sequence, e.g. it accounts for the finite and spherical shape of native protein states with the lowest free energy [36]. It should be noted, that although DOPE is not an absolute measure, it helps to rank the proposed models. Then, out of a small set of potential candidates (selection

Preprints (www.preprints.org) | NOT PEER-REVIEWED | Posted: 6 February 2019 doi:10.20944/preprints201902.0064.v1

Peer-reviewed version available at Molecules 2019, 24, 1196; doi:10.3390/molecules24071196

of 5-10), Pro-SA and ProQ analysis were used to determine the final models with the best combination of scores (**Table 1**). While for the z-score provided by ProSA-web analysis values around - 4 are suggested as acceptable, the ProQ analysis (LGscore and MaxSub) provides absolute measures. Regarding the LGscore, values > 3, for MaxSub values > 0.5 are typically considered as "good". It was observed that if secondary structural data was included using the PSIPRED webserver [37] the overall scores improved. All final DR models (**Table 1Error! Reference source not found.**) achieved LGscores > 4 and MaxSub scores > 0.5. The highest z-score was obtained for the D_4R model, whereas the lowest were counted for the D_1-like DR models. In summary, scores allowed us to move models forward towards MD simulations.

Table 1 - Metrics and scores of the DR homology models.

DR	DOPE	LGscore	LGscore +PSIPRED	MaxSub	MaxSub +PSIPRED	z-score
D_1R	-39070.82	2.53	4.26	0.18	0.53	-2.14
D_2R	-39284.66	2.52	4.22	0.21	0.52	-2.22
D_3R	-39458.37	3.14	4.19	0.27	0.55	-3.12
D_4R	-36738.05	3.33	4.25	0.25	0.59	-3.90
D_5R	-38356.05	2.60	4.14	0.15	0.57	-1.49

2.2 Molecular Dynamics Analysis

MD simulations were briefly analysed to confirm the stability of the models. Root-Mean-Square-Deviations (RMSD) mean values ranged from 0.3 nm and 0.5 nm (**Figure S1**). Overall, the five models showed good overall stability. However, D1-like models showed slightly higher RMSD values than D_2-like models: D_1R (0.48 ± 0.07 nm) and D_5R (0.49 ± 0.06 nm) vs D_2R (0.35 ± 0.09 nm), D_3R (0.34 ± 0.04 nm) and D_4R (0.36 ± 0.09 nm). This behaviour is justified by the higher homology scores attained for the D_2-like subfamily.

2.3. Ligand binding to Dopamine Receptors

In this work, we used the comprehensive review of Floresca and Schnetz (2004) [38], highly used [39–41], as a base for the definition of the binding pocket of all dopamine receptors. Furthermore, by applying Ballesteros & Weinstein numbering (B&W) [42] the position of considered important residues was more easily comparable between all receptors. Mutagenesis studies have shown that for dopamine binding, the endogenous agonist of the DR, a negatively charged aspartate (3.32Asp) is believed to form a ionic bond interaction with the protonable amine of dopamine [2,41,43]. Moreover, it was shown that this effect was crucial for ligand binding and that this amino acid was not only conserved among the DR, but also in all biogenic amine GPCRs [44,45]. Also, a serine microdomain on TM5 (5.42Ser, 5.43Ser, 5.46Ser) was

considered as an important feature for dopaminergic binding in all DRs as it is believed that the serines form hydrogenic bonds with the catechol hydroxyls of dopamine, increasing the binding affinity and orienting ligands in the orthosteric binding pocket [38,43,46–48]. While 5.42Ser seems to be critical, 5.43Ser plays a less important role [38]. A further microdomain, the aromatic microdomain, consisting of 6.48Trp, 6.51Phe, 6.52Phe and 6.55His/Asn has been reported to trigger the activation of the dopamine receptor. All amino-acids in this microdomain share the same hydrophobic face in the water-assessable binding-site crevice, indicating that any reorientation of these residues by binding to a ligand would cause steric clashes and therefore would force the residues to reorient themselves in a domino-like fashion, which lastly leads to the so-called "rotamer toggle switch" [38,41,44,49]. In addition, 6.48Trp was reported together with 6.55His to stabilize the position of the ligand in the binding pocket via π-π-stacking [38,49]. Therefore, 6.48Trp and 6.55His as well as one phenylalanine (6.51Phe) were chosen for the docking protocol to mimic the ligand-binding on TM6. Dependent on the ligand properties other residues of TM3 were also considered, such as 3.33Val and 3.36Cys. 3.36Cys is believed to be part of a deeper subpocket below the Orthosteric Binding Pocket (OBP) [29]. Additionally, Ericksen *et al.* reported that this cysteine was a relevant residue for benzamide binding [40]. Regarding 3.33Val, it was reported to show interaction with *N*-methylspiperdone by Moreira *et al.* [44] as well as with the methoxy ring of nemonapride, determined in the crystal structure of the D_4R [28]. Different authors hypothesized that DRs have a secondary binding pocket (SBP) next to the OBP [28,32,50]. Crystal structures of D_2R (PDBid: 6CM4) [29] and D_3R (PDBid: 3PBL) [32] and computational data suggest that 7.43Tyr is also a crucial amino-acid for interaction in the SBP [10,29,32]. 2.57Val was shown to form a hydrophobic pocket for antagonists like clozapine and haloperidole [48]. However, since the OBP is widely explored through experimental, computational and crystal structure data, there could be other residues important in the SBP. In order to compare all DRs ligand-binding properties and specificity, we focussed on the mentioned residues in the OBP. Detailed information about the literature (mostly regarding D_2-like DR) and which residues were chosen for docking can be reviewed in the appendix: **Figure S2, Table S2.**

2.3.1 Ligand docking

After 100 ns MD simulations of each model, 10 conformational rearrangements plus initial model (time 0 ns) were chosen for each receptor and subjected to molecular docking of 15 different ligands. It is well known that GPCRs take an infinite number of conformations over time, and this approach allows us to verify the effect of punctual fluctuations into the overall binding arrangements of ligands. The results of the molecular docking were evaluated by AutoDock4.2, which ranks the possible binding positions by energy level and clusters these positions by Root-Mean-Square-Deviation (RMSD) of 2 Å. In addition, the total number of conformations (NoC) in these clusters were counted. All results of the docking can be checked in supplementary information: **Tables S3-S7**.

Preprints (www.preprints.org) | NOT PEER-REVIEWED | Posted: 6 February 2019 doi:10.20944/preprints201902.0064.v1

Peer-reviewed version available at *Molecules* **2019**, *24*, 1196; doi:10.3390/molecules24071196

As proof of concept, redocking of the co-crystalized ligands to the crystal structure templates of the D_2R, D_3R and D_4R (PDB-ids: 6CM4 [29], 3PBL [27], 5WIU [51]) was conducted (**Figure S3, Table S8**). Receptors and ligands coordinates were retrieved from PDB files. Top clusters achieved a ligand pose equivalent to the pose in the correspondent crystal, presenting very small RMSD values. Lastly, these results were compared to the dockings of the corresponding DR-models and ligands at time point 0 ns. The binding energies of the two sets were found to be in a similar range. This is a further evidence of docking protocol reliability.

For a general overview, binding poses with more than 5 conformations per cluster were considered as a valid ligand position, despite the Binding Energy (BE) of this pose (**Figure 1A**). Regarding the docking of dopamine, it can be stated that the binding energy of D_2R was the most stable at different analysed MD conformations, while for the other subtypes it oscillated more frequently. Only at 95 ns the binding energy slightly increased up to -9.9 kcal/mol for the D_2R. For D_5R the highest binding energy was observed at 70 ns (-10.4 kcal/mol), while for the D_1R at 75 and 90 ns the binding energy was the highest (-10.8 kcal/mol). However, for D_4R the binding energy largely decreased at 90 ns to -7.3 kcal/mol. Over time the average binding energy for all DR was found to be at -9 kcal/mol.

The highest NoC during all MD conformations were obtained for D_4R and D_1R (up to > 80 for D_4R at 95 ns), while for D_2R around, 30 conformations were counted for all conformational arrangements (**Figure 1B**). Lastly, for all DRs complexed with dopamine, the first or the second cluster with the lowest binding energy also contained the highest NoC, indicating that the docking of dopamine is stable and reliable (**Table S3-S7**).

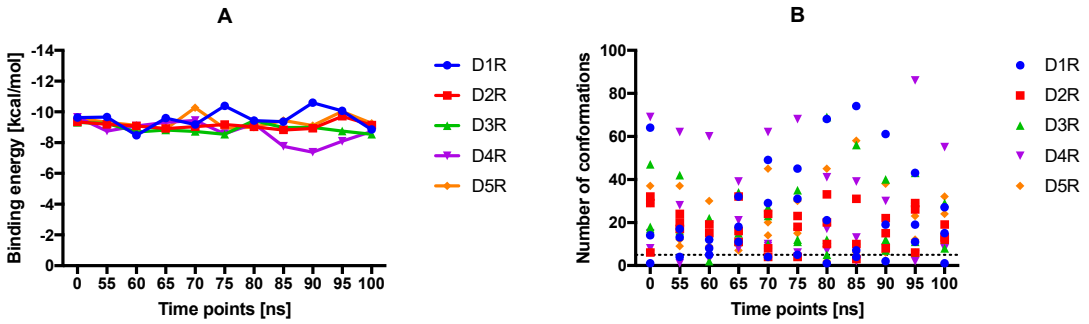

Figure 1 - Results of the molecular docking of dopamine for all DR subtypes at all MD time steps. For the binding energy (A) the mean of the 3 lowest energies of dopamine was calculated. In B the number of conformations of the three clusters with the lowest binding energies are shown for each time point and receptor.

The binding position of dopamine at all DR complexes was stable over time namely, the protonable amine was always directed towards the aspartic acid on TM3 (3.32Asp) and the hydroxy groups were facing the serine microdomain (5.42Ser, 4.32Ser and 4.46Ser), in agreement with Floresca & Schetz [38] and Durdagi *et al.* [52] (**Figures S4-S7**). As known from literature dopamine's interaction with the serine microdomain only typically requires two of the serines binding to the hydroxy

groups [38]. At 0 ns dopamine was located planar in the OBP in the above-described position. Notably, D_2R and D_4R hydroxyl groups were more directed towards serine microdomain (**Figure S4**). At 55 ns torsions were observed for dopamine bounded to all DR, which included a switch of interactions with the serines at TM5 for D_3R, since it is known that dopamine is only capable of interacting with two of the three serines [38]. At 60 ns dopamine is shifted more to the serine and aromatic microdomain (TM6) for all DRs in a different manner. However, only at D_4R a strong direction of dopamine's protonable amine towards 3.32Asp was observed. At 65 ns dopamine bounded to all DRs was located again planar in the OBP (**Figure S5**). Small individual torsions were observed during the period of 70-90 ns (**Figure S5, S6**). Interestingly, at 95 ns dopamine was strongly involved in the aromatic microdomain (TM6) at all DR, which is then vanished especially for D_3R at 100 ns. The large decrease in D_4R binding energy at 90 ns can be explained, by the approximation of dopamine to 3.32Asp and as such far away from the serine microdomain (**Figure S6**). In summary, the binding energy and 3D positions of dopamine-docking may demonstrate the binding-mode of dopamine to DRs. According to Floresca and Schetz, these features are crucial for dopamine's binding affinity and DR activation but must not necessarily be true for all dopaminergic ligands (selective and non-selective) (**Table 2**) [38].

Since non-selective agonistic activity was already covered by dopamine docking, chlorpromazine was chosen as a non-selective antagonist [53,54]. Herein, we selected the following ligands: SKF38393 as selective D_1R agonist [19,21] and SCH23390 as D_1-like DR antagonist [22,55], apomorphine as selective D_2R agonist [52], 7-OH-DPAT as selective D_3R agonist [14], nemonapride as D_2R and D_3R selective antagonist [56] and lastly haloperidole, due to its affinity for D_4R [16]. The obtained binding energies and NoC in these clusters are summarized in **Figure 2** (graphical output of the other ligands can be found in the appendix: **Figure S8**).

Preprints (www.preprints.org) | NOT PEER-REVIEWED | Posted: 6 February 2019 doi:10.20944/preprints201902.0064.v1

Peer-reviewed version available at *Molecules* **2019**, *24*, 1196; doi:10.3390/molecules24071196

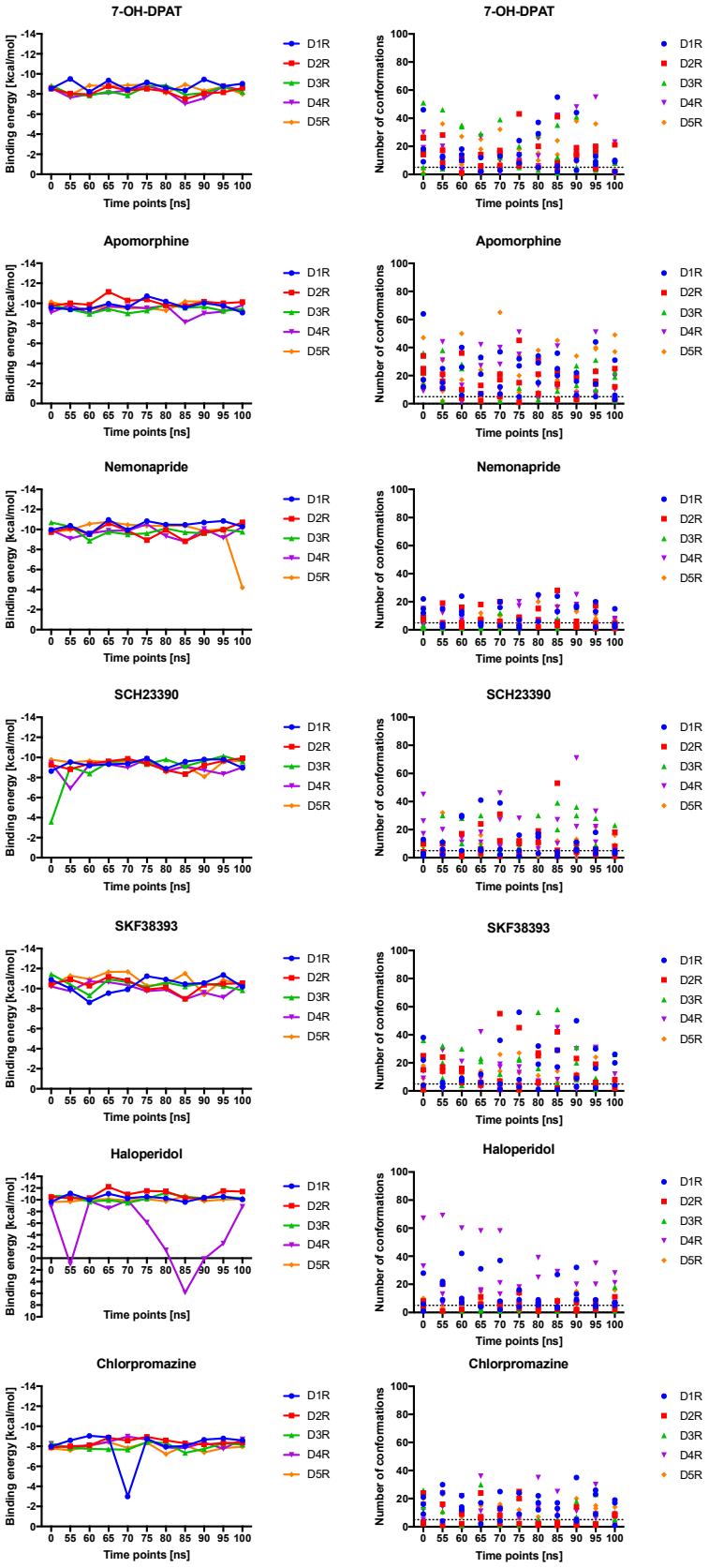

Figure 2 - Results of the molecular docking of 7-OH-DPAT, apomorphine, nemonapride, SCH23390, SKF38393, haloperidole and chlorpromazine for all DR subtypes at time points [ns]. The mean of the 3

lowest binding energies of dopamine were calculated in the left plots. The number of conformations of the three clusters with the lowest binding energies were plotted for each time point and receptor (right plot).

For 7-OH-DPAT, we observed a low and stable binding energy upon binding to all DRs. Similar to dopamine binding, the NoC decreased at all DRs from 0 to 65 ns. For apomorphine, the lowest binding energies were obtained for D_1R and D_2R. A decrease in the binding energy was determined for D_2R at 65 ns (-11 kcal/mol), whereas an increase at 85 ns was shown for D_4R (-9 kcal/mol). Similar stable binding energy around -10 kcal/mol were observed for DR:nemonapride complexes, however a massive increase was observed for the D_5R at 100 ns. In addition, lesser NoC were counted for nemonapride in total at all DRs (max. 30 at 85 ns for D_2R). For SCH23390, but not for SKF38393 the binding energy was stable over time at -9 kcal/mol for all DRs. The binding energy of SKF38393 at D_2R and D_4R increased at 85 ns. However, the NoC for SKF38393 were the lowest over 70-85 ns period for D_1R, D_2R and D_3R. Haloperidole displayed the most interesting docking-profile: while the binding energies of DRs were stable at -10 kcal/mol, only for D_4R a massive increase was observed at 55 ns and 80-90 ns into the positive range, meaning these binding positions were extremely unfavourable for haloperidole. In contrast, the NoC was found to be stable over time except for D_1R with up to 40 conformations at 60 ns. Most interestingly, most conformations were counted for the D_4R especially at 0-70 ns. Lastly, chlorpromazine binding energy experienced an increase only for D_1R at 70 ns up to -3 kcal/mol.

For further analysis, we summarized data in order to perform comparison only between ligands and receptors.

2.3.2. Distances between ligands and interacting residues

For additional evaluation of the docking performance and determination of ligand interactions within the residues of the binding pocket, the distance between the center of mass of the ligand and the alpha carbons of these residues was measured. Assuming that the time points conformations did not have an effect on the binding energy and the NoC of the ligands on the DR subtypes, the means of each ligand for all time points were calculated. Overall results of all ligand-residue measurements showed that 3.32Asp was the closest residue to all ligands for all DR subtypes, except for D_4R. In contrast the 5.42Ser was shown to be most distant at D_1R and D_2R, but not at D_5R where this was the case for 5.46Ser.

Subtype specific tendencies were nevertheless observed. The distances between the ligands and 5.43Ser was smaller compared to another binding pocket serine in D_1R, D_4R and D_5R, while this was not the case for remaining DRs. When comparing those residues to the set of residues used in the docking (**Error! Reference source not found.**), 3.32Asp showed to have the closest ligand interaction (ligand center of mass - residue alpha carbon < 6 Å), but not for all ligands at all subtypes, while other residues were more distant but all around 7-8 Å. Particularly, the distance between 3.32Asp and SKF38393 was larger at the D_3R, D_4R and D_5R. Moreover, we noted for D_4R an increase in the distance between 3.32Asp and several ligands. The distance

between SCH23390 and 3.32Asp was also slightly increased, but not for D_1R. This effect might occur due to the fact, that SCH23390 and SKF38393 are reported to be D_1R-selective [21,55].

For 7-OH-DPAT, a known D_3R selective agonist, distances between ligand and the defined pocket are higher for D_1-like receptors and distinctive residue between D_2-like seems to be 6.52Phe, that is closer to the ligand on D_3R. The same pattern was visible with apomorphine, a selective D_2R agonist, where distances in D_1-like are higher, although distinction within D_2-like family is less pronounced. Clozapine, sulpiride and risperidone are known as "dirty drugs" because of their non-selective profile, and for that reason none of these ligands showed distinctives differences between DR subtypes. Likewise, residues 3.32Asp and 3.33Val/Ile were the closest to clozapine in all five subtypes, suggesting that these residues are crucial for this ligand's binding. Haloperidole, categorized as D_2R selective antagonist with some activity on D_4R, has distinctive differences between D_1-like and D_2-like family, being closer to the second (although within D_2-like family there is no great differences on distances pattern). Spiperone and chlorpromazine have affinity for all DR subtypes, which agrees with the lack of significant differences in the measured distances. Finally, nemonapride and eticlopride, described as D_2R/D_3R selective antagonists, were located closest to the D_2-like DR residues compared to the D_1-like DR, however it seemed as these two ligands demonstrated preference for the D_4R.

With reference to the conserved amino acids of the DR binding pocket: 3.32Asp, 5.42Ser, 5.43Ser, 5.46Ser and 6.48Ser, we observed certain ligand and receptor specific differences in binding (measured in distance between ligand and residues). One must take into consideration that for the docking set-up, we choose specific residues that are believed to form meaningful interactions. Another point to consider is the size and affinity for the ligands at these receptors. As such, ligand-based analysis was applied to address ligand properties unbiased (which is the case for applying flexible residues in the molecular docking approach) towards the receptor's structural properties.

Preprints (www.preprints.org) | NOT PEER-REVIEWED | Posted: 6 February 2019 doi:10.20944/preprints201902.0064.v1

Peer-reviewed version available at Molecules 2019, 24, 1196; doi:10.3390/molecules24071196

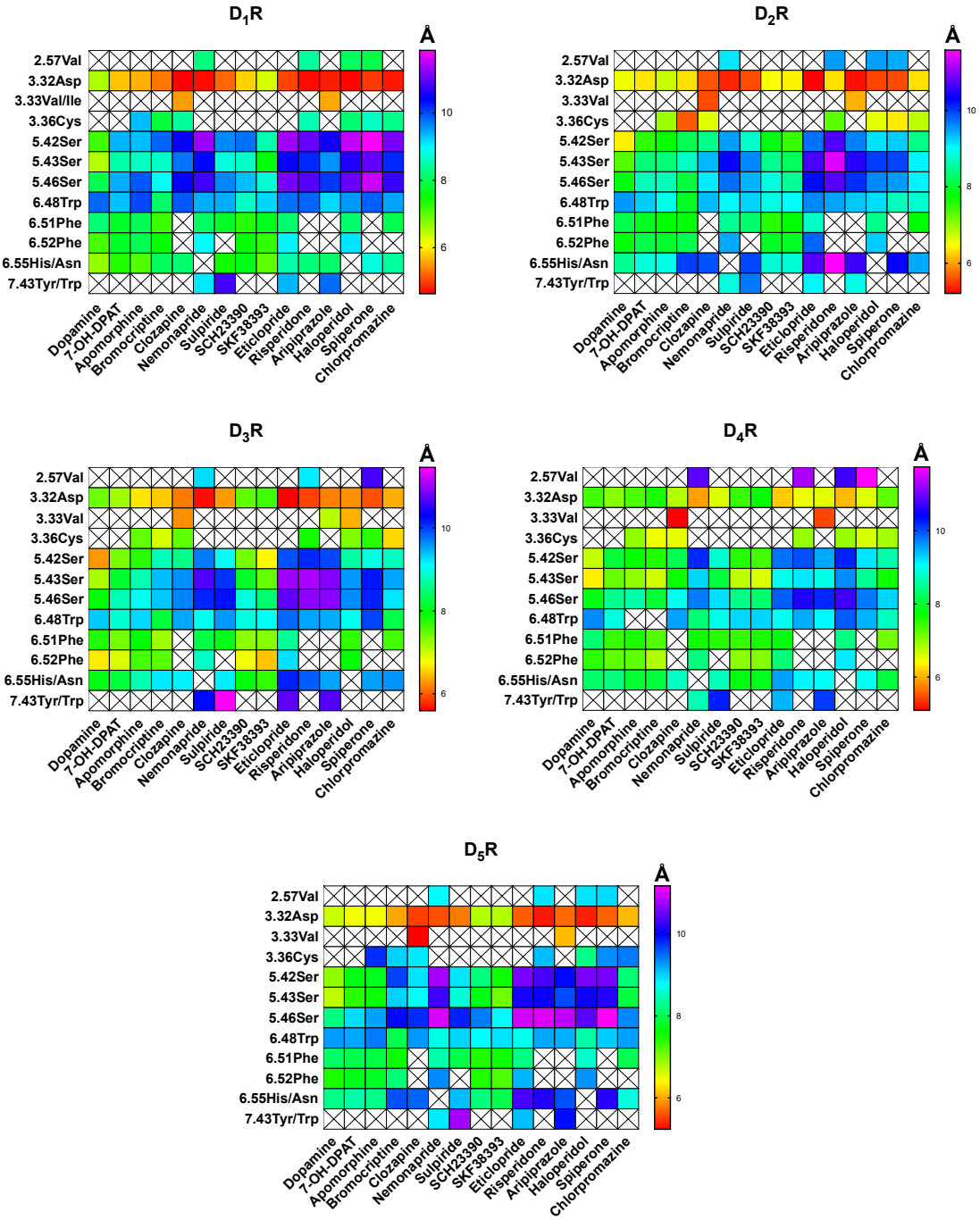

Figure 3 - Summary of the distances between ligands and residues used in molecular docking for all DR subtypes. For each ligand-residue-distance [Å], we calculated the mean of all time points of the conformational models (11) of the three best docked clusters ranked by binding energy [kcal/mol] Noteworthy is that not all ligands were set to interact with all residues shown in the x-axis in the molecular docking. (e.g. only clozapine and aripiprazole were set to interact with 3.33Val). Distances below 6 Å are coloured red, while distances > 10 Å are coloured blue-violet.

2.3.3. Pairwise interactions

In-house scripts using the BINANA algorithm were constructed to identify the type of interactions established between the ligands and all DRs [30]. Close contacts between receptor and ligands were measured at 2.5 and 4.0 Å. Moreover, it also allows the determination of hydrogen bonds (HB), hydrophobic contacts (hydrocontacts) and salt-bridges (SB) as well as π-interactions, further subdivided into cation-π-interactions (cat-π), aromatic superpositions (π-π-stack) and perpendicular interactions of aromatic rings also referred to as edge-face-interactions (T-stack) [30]. For a first overview, all interactions despite their type and ligand were summarized and compared between the DR-subtypes (**Figure S9**)

On average, majority of interactions were found for D_4R (around 3686 ± 377), concentrated at the conformation arrangement found at time point 95 ns. Similar trend was observed for the D_1R (average of total interactions 3257 ± 209), where the maximum NoC was counted at 100 ns, while for the other DRs the interactions slightly decreased at the end of the MD simulation conformation. Least interactions in total were found with the D_5R (2793 ± 170), while the D_2R counted 3037 ± 210 and the D_3R 2893 ± 175 total interactions, on average. We found the lowest number of interactions at 80 ns (2903 ± 295), whereas the highest were counted at 95 ns (3408 ± 523).

In a more detailed look, the number of 4 Å-interactions, as expected due to the possible involvement of a higher number of atoms, and consequently hydrocontacts are the most frequent (around 75 to more than 100) over time, when compared to all other interactions ranging from 50 to 0 for all ligands at all DRs (**Figure 4Error! Reference source not found.**). In addition, the number of contacts was found mostly for D_4R and the smallest number for D_3R and D_5R (4 Å-contacts). Hydrocontacts contacts were counted mostly for D_1R and lastly for D_3R. Per interaction type, as also expected by comparison with other systems, the smallest number of interactions were counted for cat-π-interactions and hydrogen bonds, which ranged between 0 and 2 contacts. Dopamine, due to its small size, established the lowest number of contacts when bounded to all DRs. On the contrary, bromocriptine seemed to form the highest number. Bromocriptine was also the only ligand with hydrocontacts > 100 at $D_{1\text{-}4}R$, while 97 were counted for D_5R. Only D_4R risperidone and spiperone showed hydrocontacts in similar ranges (59 and 62 respectively). Lastly, for each ligand a similar pattern with slight variations was found for each DR. For apomorphine, 10 T-stacking interactions were always formed for D2-like DR, while only 6 were found for D_1R and 12 for D_5R. Bromocriptine had the most discrepancies at 2.5 Å-number of interactions: highest number found at the D_4R (31) and least at D_5R (8), while it did not differ much for the other DRs. We stress out that for clozapine, risperidone and aripiprazole, no cat-π-interactions could be identified at the D1-like DR. In addition, for risperidone, more hydrocontacts were found at the D_1R and D_4R (70, 80) compared to the other DRs (2x 54, 59). Furthermore π-π-stacking was favoured at the D_3R (8 contacts), while for D_1R and D_2R 2 contacts were found, and for D_4R and D_5R 4 π-π-stacking interactions were found. For

Preprints (www.preprints.org) | NOT PEER-REVIEWED | Posted: 6 February 2019 doi:10.20944/preprints201902.0064.v1

Peer-reviewed version available at Molecules 2019, 24, 1196; doi:10.3390/molecules24071196

aripiprazole, a D_1R and D_4R preference was found for 4 Å-interactions and hydrocontacts compared to the other DRs (lower contacts in the inner sphere), while for spiperone a distinctly decrease in contacts for these interaction types was observed for D_3R. Lastly, for chlorpromazine, the lowest number of 4 Å-interactions was found for D_5R, while in contrast most T-stacking interactions were found for this DR-subtype. **Figures S10-S24** show a closer detailed of the change of interaction-pattern over time.

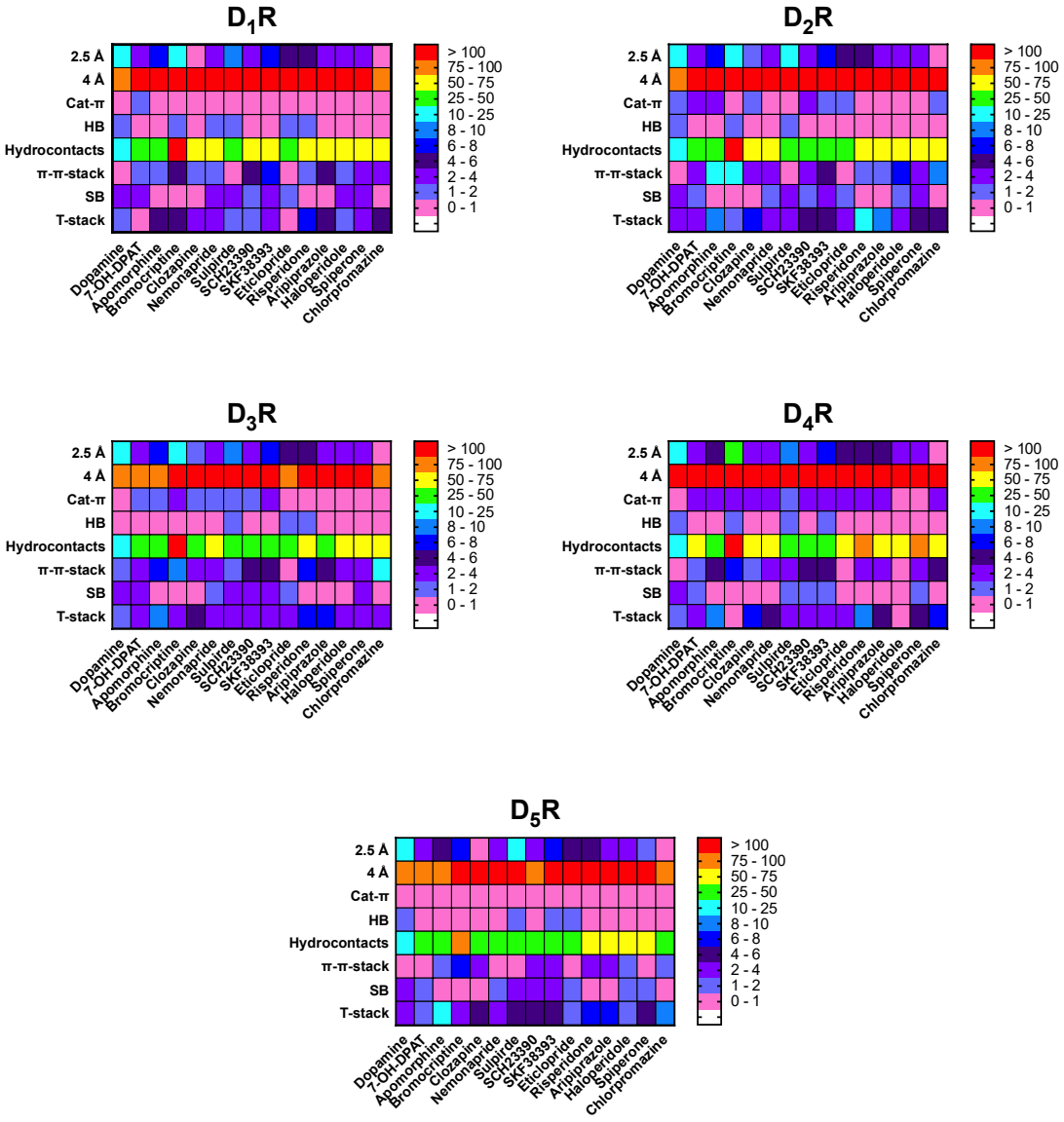

Figure 4 - Interactions types counted for each ligand at DR-subtypes. The data is summarized for each ligand at all time points. Total numbers of the contacts for each interaction type are color-coded: Red stands for > 100 contacts, orange 75-100, yellow 50-75, green 25-50, cyan 10-25, light-blue 8-10, dark-blue 6-8, dark violet 4-6, violet 2-4, light violet 1-2 and pink indicates when 0 contacts were counted. White cells indicate that these values are outside the scale.

2.5 Å interactions

2.5 Å-interactions, very short (closer) contacts are especially relevant for ligand binding. For dopamine the number of these interactions increased for D1-like DRs at 95 ns, while for 7-OH-DPAT the highest number of interactions observed in total only occurred for D_3R (counting highest at 95 ns). For bromocriptine 2.5 Å-interactions were significantly higher for D_4R. This effect was also observed for clozapine with (counting highest at 95 ns). Also, haloperidole seemed to have a higher number of established interactions with D_4R as well as eticlopride, for which the most interactions were observed at 65 ns. Only risperidone had a higher number of interactions with D_2R, especially at 95 ns. Regarding the D_1-like DRs, nemonapride established the majority of D_1R at 80 ns and sulpiride for D_5R at 95 ns. Chlorpromazine had the lowest number of compared to all ligands with no preference for any DR-subtype. All in all, the 2.5 Å-interactions seemed to be particularly relevant for the ligand binding to D_4R.

4 Å-interactions

Contrary to 2.5 Å-interactions that show higher specificity, 4 Å-interactions are more unspecific but may reveal other indirect receptor-ligand contacts. Bromocriptine showed the highest number of 4 Å-interactions (> 200) among all DRs since it was also the most ornate ligand. In addition, less hydrocontacts were found at the D_2R, D_3R and D_5R compared to the other DR-subtypes. Furthermore, many interactions were observed at the D_4R at 65 ns and 95 ns which is surprising as the binding energy decreases at these exact time points. Most 4 Å-interactions were found for dopamine binding to D_1R, while for apomorphine this was the case for D_4R. Nemonapride showed a high and stable number of interactions for D_1R and D_4R binding over time, yet a decrease in interaction was found for D_5R at 100 ns. SCH23390 displayed a preference for D_4R, especially at 95 ns. Also, aripiprazole seemed to favour 4 Å-interactions preferably with the D_4R despite a high interaction-loss at 90 ns. Once again, 4 Å-interactions are higher in D_4R:ligand complexes.

Cat-π-interactions and π-π-stack

Cationic-π and π-π-stacking are considered as natural key non-covalent interactions [57]. They are important as solitary effects, but also their interplay omnipresent in many biological systems [58]. In the DR-ligand system frequent oscillations between time points was noted for some ligands. Dopamine, for example, showed highest cat-π-interactions for D_2R but this oscillated from 2-4 interactions/time point. π-π-stacking interactions displayed a similar pattern. 7-OH-DPAT showed a variety of possible cat-π-interactions and π-π-stack at the D_5R. Apomorphine demonstrated cat-π-interactions between 55 and 75 ns with D_5R and π-π-stacking-interactions with D_2R between 60 and 80 ns. Bromocriptine displayed a wide array of cat-π-interactions per time point (0-6 interactions) with D_2R and D_3R. In contrast none were found for D_1R complexes. π-π-stackings occurred with bromocriptine and D_5R

between 85 and 100 ns. Clozapine showed also no cat-π-interactions with D_1R. Nemonapride showed oscillating π-π-stacking-interactions without preference for one particular DR. However, a lot of cat-π-interactions were counted for D_5R between 70-80 ns. For risperidone, cat-π-interactions were mainly formed with D_4R, while π-π-stacking was mostly related to D_3R complexes. Aripiprazole seemed to preferably form cat-π-interactions with D_4R, while increasing π-π-stacking-interactions were observed with D_1R between 65 and 80 ns. Haloperidole seemed to prefer π-π-stacking-interactions with D_2R, maybe important for its selectivity towards this receptor. For chlorpromazine, no cat-π-interactions were observed at D1-like DRs (D_1R and D_5R), while many interactions were counted with D_2R between 65 and 75 ns, with D_3R at 95 ns and with D_4R at 60 ns.

T-stacking

The T-stacking-interactions were similar to cat-π- and π-π-interactions, yet more frequent fluctuations in the number of interacts between ligands and receptor were observed in total. Especially for risperidone, which showed the highest number of T-stacking-contacts, preferably with D_2R. Haloperidole and spiperone also seemed to have a D_2R-preference, while chlorpromazine formed a large number of interactions with D_5R. In brief, our results also pinpoint for the fact that T-stacking-interactions seem to be relevant for large ligands, primary in antagonists binding than in agonists case.

Salt-bridges

The following ligands did not form any salt-bridges at any time point: apomorphine, bromocriptine, clozapine, risperidone, aripiprazole and chlorpromazine. Most stable salt-bridge bonding at all DR-subtypes was unsurprisingly achieved by dopamine. 7-OH-DPAT salt-bridge-bonding was found for D_1R (3 in total), while for the other subtypes, contacts ranged between 1 and 3 over time. The same trend was observed for nemonapride and SKF38393. SCH23390 formed the highest number of salt-bridges with D_5R and with D_2R between 70 and 85 ns. Haloperidole seemed to establish a higher number of salt-bridges with D1-like DR and D_2R, while none were formed with D_3R and D_4R. Spiperone seemed to preferably form salt-bridges with D1-like DRs.

Hydrogen bonds and hydrophobic contacts

Charge-reinforced hydrogen bonds are reported to be much stronger than the neutral hydrophobic contacts [59]. Moreover, it was reported that Hydrogen Bonds (HB) determine the specificity of receptor-ligand binding [59]. Hydrophobic contacts (hydrocontacts) also contribute to ligand-binding, and a balance between HB and hydrocontacts is required for drug-like molecules [59]. Therefore, it was not surprising that a large number of hydrocontacts was observed for all ligands, while HB were less common. Hydrocontacts were found for dopamine binding to D1-like DRs between 60 and 70 ns; while HB were only formed with D_1R during this time period. Not more than 2 HB were found at any DR bounded to 7-OH-DPAT, while

hydrocontacts were preferably formed for D_1R between 60 and 70 ns. Bromocriptine seemed to build a large hydrophobic network with the D_4R at 65 ns, while this was the case for clozapine during 85 to 100 ns. Aripiprazole was found to form steady number of hydrocontacts at D_1R while increasing hydrocontacts were found at the D_4R at 90 ns. Inversely the number of hydrocontacts with the D_2R, D_3R and D_5R decreased at that time point. Lastly, chlorpromazine seemed not to form any HB at any DR complex. In brief, D_1R and D_4R showed similar interaction-patterns, distinguishing themselves from the rest of DRs.

Furthermore, the pairwise analysis resulted in the key receptor residues, responsible for the establishment of these types of interactions. By assorting those for each ligand at all DRs (time points summarized), patterns but also unique receptor-ligand interactions were visible (**Tables S9-S13**). Notably for this part of analysis the 4 Å-interactions were omitted as they were found to be unspecific and occur very frequently.

Conspicuously, residues on TM4 were not contributing to receptor-ligand interaction except at D_4R complexes. It was not surprising that the "classical" TMs, e.g. TM3, TM5, TM6 and TM7 were involved in many different interaction types. By comparing large ligands such as spiperone or haloperidole with rather compact ligands such as dopamine, SCH23390 or clozapine, it was possible to point out a larger number of TM1 and TM2 residues involved in establishing meaningful interactions. Author's had already hypothesized that these residues could belong to a secondary binding pocket, only accessed by large ligands [48,60].

Undoubtedly, 3.32Asp was always involved in the establishment of salt-bridges for all DRs. However, at D_1R, 74Pro located on ECL1 appeared also to establish salt-bridges. In addition, D_3R salt-bridge-bonding for spiperone was found occur with 1.44Leu and 75Ser (ECL1) rather than with 3.32Asp. All in all, salt-bridges were found to be highly conserved regarding the residues involved. In contrast, most interactions in total and most unique interactions were found within hydrocontacts (hydrophobic bonds). Especially bromocriptine displayed the most divergent hydrophobic network at all DR ranging from conserved and non-conserved residues involving all TMs.

Most interesting were the HB interactions. For dopamine a different set-up was presented at each DR. While the D2-like DRs and D_5R HB were formed by the serine microdomain (5.42Ser, 5.43Ser and 5.46Ser), for D_1R the serine microdomain was not involved at all. 3.32Asp appeared as interaction partner for all DRs. At D_5R, an HB with 5.38Tyr and dopamine was unique for this interaction type for all ligands. However, 5.38Tyr was found at the D_4R to form HB with 7-OH-DPAT.

Less cat-π-interactions were found at the D_5R and not for all ligands, while most were found at the D_3R. Only bromocriptine (3.28Trp, 6.51Phe), nemonapride (6.48Trp, 6.51Phe, 6.52Phe), sulpiride (2.61Lys, 6.48Trp, 6.51Phe) and SCH23390 (6.48Trp) showed cat-π-contacts at the D_5R. Also, at the D_1R cat-π-interactions were less common and mainly formed by conserved residues on TM6 (6.42Gly, 6.31Thr, 6.30Glu, 6.39Val). Interestingly for dopamine at D2-like DRs most 6.55His was

involved in HB interactions, moreover at the D_4R this interaction type occurred only at time point 65 ns. The same effect was found for clozapine for D_2R.

T-stacking-interactions were found for almost all ligands when complexed to all DRs, except for bromocriptine and sulpiride at D_2R, haloperidole at D_4R and spiperone at D_5R. It was also visible that most T-stack-contacts were counted for D_3R and less for the D_5R in general. T-stack-contacts were mainly formed, despite the ligand, by residues either from the aromatic microdomain (6.48Trp, 6.51Phe, 6.52Phe, 6.55His), but also by other conserved residues (6.39Val, 6.42Gly, 6.43Val). Unique interactions were found for risperidone at D_4R with 6.44Phe and for chlorpromazine at D_1R with 6.30Glu. However, other residues from other TMs were also involved in forming T-stack-contacts: for example, 7-OH-DPAT unique interaction with 2.47Ala and for SKF38393 with 35Ala (ICL1) were found at D_3R. For risperidone another unique interaction with 231Phe (ICL3) was determined at D_1R. While for spiperone 1.35Tyr and 159Ile (ECL2) seemed to be relevant for D_4R. For chlorpromazine, 2.14Tyr was relevant in D_4R coupling. TM7 residues were participating in T-stack-formation, such as 7.34Thr (D_1R) and 7.35Tyr (D_2-like)/7.35Phe(D_5R), 7.43Tyr(D_2-like), which was more frequently observed for D_2-like DR-subtypes. Residues on TM2 were also relevant for T-stack-formation (2.41Tyr, 2.43Val, 2.45Ser, 2.46Leu, 2.47Ala, 2.50Asp) but only for D_3R. For D_4R and D_5R, only residues from TM6 and TM7 were involved in T-stack-contacts, except for SKF38393 where 5.47Phe was relevant for binding to D_4R. Lastly, for D_1R and D_2R TM3 (3.28Trp(D_1R)/3.28Phe(D_2R)) residues also established meaningful interactions with nemonapride, sulpiride, SCH23390, aripiprazole and spiperone.

Although these residues (especially on TM2 and TM7) are more related to the SBP than to the OBP (herein TM6 is the most relevant TM), contact formation was also observed for smaller ligands (7OH-DPAT, SCH23390, SKF38393). It was not expected that these ligands would access the SBP. Noteworthy is also the fact, that dopamine exclusively formed T-stack-contacts with the conserved aromatic microdomain at all DR. Lastly, contacts with residues from TM6 were found highly relevant for all ligands and all DRs. Finally, it was also obvious that the variety of T-stack-contacts was also limited by the number of aromatic rings of the ligand (e.g. dopamine only contacted 3 different sequential residues).

The π-π-interactions were rather rare compared to the other interaction types. Here, the least contacts were found for D1-like DR subtypes, while most were found at the D2-like subtypes, and in particular for D_3R. Some ligands did not form π-π-stacking interactions with DR subtypes (e.g. none π-π-stacking were found for D_1R binding to dopamine, 7-OH-PAT and sulpiride; D_2R was not favoured by sulpiride either). Eticlopride and haloperidole were not attracted by residues on the D_4R, while nemonapride did not favour π-π-stacking with D_5R. It was also obvious, that similar to T-stacking, the residues of the aromatic microdomain (6.48Trp, 6.51Phe, 6.52Phe, 6.55His) were responsible for the majority of ligands interactions to all DRs. However, different residue partners were determined for π-π- compared to T-stacking such as residues from TM5 (5.38Tyr, 5.47Phe). For aripiprazole, residues 7.43Tyr (D_2R-D_4R) and 7.34Thr (D_1R) seemed also to be important for this type of

interaction. Most interesting was the interaction pattern for sulpiride: while for D_1R and D_2R no π-π-stacking was detected, for D_3R and D_5R only a few residues seemed to be relevant (2.43Val, 2.44Val, 2.48Val, 38Thr, 5.38Phe, 6.51Phe, 6.52Phe for D_3R; 3.28Trp and 6.48Trp for D_5R) while for D_4R, 27 residues from all TMs were involved in contact network formation. This may be explained by the different possible binding poses of sulpiride on the different D_4R conformations.

3. Discussion

3.1. Homology modeling

Homology modeling of all DR subtypes showed that there were smaller structural differences among the "classical" TMs (TM3, TM5, TM6), which are important for ligand binding. Yet, as expected, structural differences between the subtypes were observed in the intracellular and extracellular loops, where some are important for ligand binding (ECL2) or for intracellular signalling (ICL2) [61]. The latter was the case for the D_1-like, due to its larger intracellular loop 3. The combination of MODELLER [32] ClustalOmega (used for multiple sequence alignment [36] provided suitable models for molecular docking and is a straightforward protocol to follow. Although no crystal structure is available for the D1-like DRs, the high sequence similarity among all DR helped to find suitable models for molecular docking.

3.2. Model metrics

There are several approaches to validate homology models such as built-in metrics of open-source [43] and licensed softwares [62]. In a preliminary study we experienced [41] that the combination of different independent metrics provided adequate models suitable for molecular docking. For instance, the combination of MODELLER's metrics [31], ProSA-web [63,64] and ProQ [65] revealed to be promising and again straightforward. We could not compare our models with other authors as metrics scores are mostly not shown [63,66]. D_1-like models, which did not have their own crystal structure template and D_2-like models for which its own crystal structure templates are available showed similar quality. In conclusion, the homology modeling approach and evaluation using the MODELLER's metrics, ProSA- and ProQ-analysis is a promising and reliable protocol to create valid models for molecular docking.

3.3. Molecular docking and definition of the binding pocket

In general, the docking performance of the DR homology models and the ligand-set seemed to be reproducible, low binding energies, high NoC by cluster and no significant differences were found for the 11 conformational rearrangements tested. Certainly, ligand specific differences were observed. For example, dopamine constantly showed the lowest binding energies combined with the highest NoC per cluster, whereas haloperidole's binding energies were even lower but rarely with

Preprints (www.preprints.org) | NOT PEER-REVIEWED | Posted: 6 February 2019 doi:10.20944/preprints201902.0064.v1

Peer-reviewed version available at Molecules 2019, 24, 1196; doi:10.3390/molecules24071196

over 10 conformations. Bromocriptine was an exception throughout the docking processes as it expressed positive binding energies, indicators of an unfavorable position of the ligand in the receptor. However, since bromocriptine acts as an agonist for DRs, is was expected that binding properties would be similar as for other agonists and dopamine, which was chosen in this large study. In other studies where the active state of the D_2R was investigated, lower binding energies were measured maybe due to differences in the used templates (here we used the most recent one, D_2R itself) [52]. However, Sukalovic *et al.*, who used D_3R crystal structure as template for D_2R modeling, and then docked their own synthesized dopaminergic arylpiperazines, attained binding energies around -10 kcal/mol, in line with our results [60]. The binding pocket was defined according to previous studies from literature [41]. Foremost, 3.32Asp, a serine microdomain (5.42Ser, 5.43Ser, 5.46Ser) and an aromatic domain in TM6 (6.48Trp, 6.51Phe, 6.52Phe, 6.55His) are believed to be crucial for dopaminergic binding and receptor activation [38]. These residues appeared to be omnipresent in all of analyses such as ligand-residue-distance- and pairwise-analyses.

3.4. Distances

A current method to access possible receptor-ligand binding properties, is the measurement of the distance between the alpha carbon atoms of the relevant residues in the binding pocket and the centre of mass of the ligands [2]. Overall, most of measured residue-ligand distances were above 5 Å. By using this approach, one can quantify the modes of interaction of these particular ligands, but otherwise one overlooks other possible meaningful residues. Yet, the distances for the most conserved OBP residues (3.32Asp, serine residues and 6.48Trp), distinct differences were observed between agonists and antagonists. For example, dopamine was constantly close to OBP, indicating it's receptor activating properties as described by Floresca and Schetz [38], while risperidone was found distant from these residues according to its antagonistic properties. This was also the case for the other antagonists such as haloperidole, nemonapride and the biased ligand aripiprazole. In addition, it may also be possible that other residues in other TMs were involved in binding of these ligands as described by Kalani *et al.* for the D_2R. [48]. Therefore, the pairwise interactions were further analysed, to gain a more detailed knowledge about ligand-binding possibilities within the DR binding pocket

3.5. Pairwise interactions

BINANA (used in other non-GPCR studies [30,67–70]*)* revealed to be a helpful tool for assessing the full binding capacity of the DRs regarding the chosen ligand set. First of all, it was visible by considering the total number of interactions per ligand that no clear D_1- or D_2-like specificity was observed, except for apomorphine (differences of 20 interactions between D_1-like and D_2-like). In total, the highest number of interactions was found for D_4R. Moreover, the lowest number of

interactions were formed with D_5R, but not with the D_1R. It was found that either D_1R together with D_4R formed the highest number of interactions with dopamine, nemonapride, eticlopride and aripiprazole. For other ligands, when this scenario occurred, the lowest number of interactions were found for D_3R and D_5R (clozapine, sulpiride, eticloride, risperidone, aripiprazole, spiperone, chlorpromazine). This cannot be related to the type of ligand, as they are all structurally diverse. Only chlorpromazine was reported to show a significantly different binding mode which was already described by Kalani *et al.* that concluded that this antagonist would have "atypical-bound-system" for D_2R [48,71]. However, for SCH23390 and SKF38393 no subtype-specific differences were observed although SCH23390 is an antagonist at the D_1-like DRs and SKF38393 a selective D_1R-agonist [72,73]. Lastly, haloperidole showed a higher number of interactions with D_4R while the number of interactions was indifferent of the other DRs. The interactions are on one hand classified unspecific in 4 or 2.5 Å radiuses or specific in the following categories: salt-bridges, hydrogen bonds, hydrophobic contacts (hydrocontacts), cation-π, π-π- and T-stack-interactions. A systematic study by De Freitas and Schapira [74] showed that the most frequent type of non-covalent interactions for protein-ligand complexes are hydrophobic contacts, followed by hydrogen bonding, π-stacking, salt-bridges, amide-stacking (corresponds to T-stack) and lastly cation-π-stacking. The same ranking of frequency of interaction type was found in our study. As also described by Davis and Teague [59] hydrophobic contacts are the most common type of receptor-ligand-interactions as they not only enhance binding affinity but also are sometimes favoured over tight, charged hydrogen bonds [59]. In addition, they can be formed with different ligand-atoms such as carbons, halogens or sulphurs [74]. As the usual cut-off for hydrophobic contacts it 4 Å, it was also not surprising that almost the same number of contacts were found in the unspecific 4 Å- analysis, whereas significantly less contacts were found within the 2.5 Å-cluster. As reviewed in Davis and Teague [59] most docking studies fail to count in the hydrophobicity for their ligands. However, the balance between polarity (causing hydrogen bonds) and lipophicity (causing hydrophobic contacts) is the main drive to make a ligand "drug-like" [59]. Our study was successful to determine not only the hydrogen bonds but also the large hydrophobic network of each "drug-like" ligand (as well as of the marketed drugs). To what extent these hydrophobic contacts contribute to ligand-binding should be further validated as suggested by Davis and Teague [59]. These hydrophobic networks were found to be scattered over residues of all TMs for all DRs. Floresca and Schetz [38] also reported that conserved residues in the OBP clustered in microdomains contribute to stabilizing ligand-binding through the formation of a H-bond network. Moreover, HBs where mostly mediated by the serine microdomain (5.42Ser, 5.34Ser and 5.46Ser especially at D_2R and D_5R). Interestingly these residues were not relevant for D_1R, although a study by Hugo *et al.* mentioned 5.46Ser as key residue for activating D_1R [75]. In this study, 3.37Trp was also proposed to be mediator of the D_1R-activation [75]. We were not able to confirm these findings in our study, only bromocriptine and spiperone were interacting 3.37Trp at D_1R, while at D_5R we did not observe any interaction with this

Preprints (www.preprints.org) | NOT PEER-REVIEWED | Posted: 6 February 2019 doi:10.20944/preprints201902.0064.v1

Peer-reviewed version available at Molecules 2019, 24, 1196; doi:10.3390/molecules24071196

residue. 3.37Thr D_2R was found to interact with 7-OH-DPAT, indicating that these residues may not be D_1R-specific. Other residues on TM3 such as 3.35Cys, 3.36Ser, 3.33Val or 3.33Ile and 3.39Ser were often found forming different interactions with different ligands. This was also in concordance with previous studies regarding the involvement of other conserved residues on TM2 and TM7 (and TM3) [48,60,76,77], which was also described as part of a SBP only assessable for ligands with piperazine-moieties [50]. Furthermore, there was a clear higher network contact formation with D_4R. Except for that fact that the D_4R is physiologically distant compared to the D_2R and D_3R, no further explanation could be found for this trend [76].

Frontera *et al.* reported that the strength of ion-π-interactions is also influenced by the presence of weaker interactions such as hydrogen or hydrophobic bonds [58]. For instance, it is well known that H-bonding is highly contributing to the bond strength of π-stacking [58]. But not only weaker interactions benefit π-interactions, cat-π and π-π-stacking were also found to be cooperative for each other [58]. Such combinations where cat-π and π-π-stacking were simultaneously present, were indisputably found at the D2-like rather than at D1-like DRs. In addition, these residues and those of the TM6 aromatic microdomain (6.48Trp, 6.51Phe, 6.52Phe, 6.55His/Asn) were mostly involved in forming π-interactions (cat-π, π-π or T-stack). This can be explained by the fact that especially amino-acids like Phe, Tyr and Trp provide a surface of negative electrostatic potential that can bind to cations through electrostatic interaction [58]. Moreover, the majority of interacting residues filtered for these three interaction types were also found to be these three types of amino acids. D_5R π-stacking-formation always involved Phe, Tyr and Trp. Therefore, these interactions with Phe, Tyr, Trp could be further extended in order to design a new selective SAR for D1-like DR ligand. Since for the D1R-like DR SCH23390 and SKF38393 are the only selective ligands so far, a closer look at the interacting residues of these ligands revealed that cat–π-interactions (6.30Glu, 6.39Val, 6.42Gly) were only present at the D_1R for SCH23390, the antagonist at the D1-like DR [73]. Moreover, these residues were rather not the "classical" TM6 residues usually involved in binding, whereas this was true for the other ligands. This encouraged the search for D_5R-selective ligands which should ideally form cat-π-interactions, as they were found in this ligand set. From a structural basis SCH23390 and SKF38393 are more related to the benzodiazepines, compared to the other ligands which are either small molecules or longer ligands with piperidine moieties [78]. Lastly, another difference found between SCH23390 and SKF38393 binding to D_5R were that SKF38393 established more interactions with residues from different TMs and a variety of neighbouring residues of the "classical" interacting residues; whereas SCH23390-receptor-interactions were more limited to a smaller number of residues. These observations were not found for both ligands at the D_1R. Reported by Bourne, who discovered SCH23390, this compound is the 3-methyl, 7-chloro analogue of the D1 agonist SKF38393, which is furthermore enantioselective [73]. In addition, it was stated that the phenyl ring in the benzodiazepine-derivatives and the receptors was

Preprints (www.preprints.org) | NOT PEER-REVIEWED | Posted: 6 February 2019 doi:10.20944/preprints201902.0064.v1

Peer-reviewed version available at Molecules 2019, 24, 1196; doi:10.3390/molecules24071196

involved in electrostatic forces, important for binding [73,79]. Mapping the full electrostatic potential of the D_5R using ligands with benzodiazepine properties may be useful to find D_5R-selective SAR.

Conclusions

Herein, we present a comprehensive *in silico* approach, to inspect protein-ligand interactions within DRs bounded to 15 ligands. One of the major research efforts in the research of dopamine receptors is the design of DR-subtype selective ligands [76]. However, most predictive studies have been performed on D_2R ligand specificity, as this receptor is the most crucial in neurotransmission [48,77,80]. Our study reveals important interactions between DRs key residues and ligands in a more detailed way when compared with available literature [46,48,50,52,60,71] Data is also in line with experimental information, which corroborates the conceptual framework of this analysis protocol [38]. DRs classical residues participate in forming contacts with all ligands (e.g. 3.32Asp undoubted forms salt-bridges with agonists, dopamine, 7-OH-DPAT, and antagonists, risperidone). Also, hydrogen-bonds were mostly formed by the aromatic microdomain of TM6. In addition, dependent on the ligand, these interaction types were either present at the DRs or completely non-existent.

A clear D_2-like selectivity or binding preference was only found for apomorphine, while for others either D_2R and D_5R seemed to form a lower number of 4 Å-interactions such as nemonapride (D_2R/D_3R-antagonist [81]), SCH23390 (D_1-like antagonist [73]), SKF38393 (D_1R-antagonist [21]) or D_1R and D_4R were highly preferred (higher number of meaningful interactions). In other cases such as for eticlopride (D_2R/D_3R antagonist [27]) and spiperone (D_2R-antagonist [56]), the D_3R was the least attractive DR for interaction. It was also shown that the NoC does not automatically result in the lowest binding energy (BE), which was most visible for haloperidole bounded to D_4R. For most ligands, a high NoC resulted in a higher number of interactions, mostly 4 Å-interactions or hydrocontacts, which points to a higher number of interactions involving the outer residue network of the DRs binding crevice when the ligand is involved in deeper conformational exploration. Regarding the electrostatic interactions, it can be concluded that they mostly contribute for a more specific binding and should therefore be closely investigated during ligand design. T-stacking interactions for D_5R were most likely to achieve the lowest binding energies. This was also true for the D_1-like DR selective ligands SCH23390 and SKF38393[78,82]. For bromocriptine, D_5R was the only DRs with negative binding energies in average. Lastly, T-stacking interactions revealed as especially relevant for some large ligands such as apomorphine, risperidone or aripiprazole.

In order to find future SARs for DRs, this computational approach helped to understand which types of interactions are major binding contributors and should be considered. Finally, this study also showed that scores made by molecular

Peer-reviewed version available at Molecules 2019, 24, 1196; doi:10.3390/molecules24071196

docking studies such as NoC and binding energy give hints but are not able to assess the full-scale binding properties and potential of a certain compound.

4. Materials and Methods

4.1. Homology modeling

4.1.1. General approach

The inactive DR models were generated with MODELLER 9.19 [31], using the D_2R complexed with risperidone (PDBid: 6CM4) [29], the D_3R complexed with D_2R-antagonist eticlopride, (PDBid: 3PBL) [27] or D_4R complexed with D2R/D3R-antagonist nemonapride (PDBid: 5WIU) [28] as templates. Depending on the sequence similarity obtained with Basic Local Alignment Search Tool (BLAST) [34] and ClustalOmega [35], either D_3R or D_4R was chosen as template to model the DR (more detailed in results section). The crystal structure of D_2R was chosen as template to model this receptor. Due to the length of the IntraCellular Loop 3 (ICL3), this was cut and substituted with four alanine residues. Water and co-crystalized compounds were removed from the template structures. In the modeling protocol the lengths of the TMs and the perimembrane intracellular helix (HX8) were specified. In addition, disulphide bonds were constricted in the known pairs of cysteines, in particular between 3.25Cys and a non-conserved cysteine in ECL2 and between two non-conserved cysteines in the ECL3. Furthermore, loop refinement was performed for extracellular and intracellular loops for all DR using the module "loop refinement" of MODELLER 9.19. The number of models calculated with MODELLER [31] was set to 100.

4.1.2 Model evaluation/ Methods of quality

We used MODELLER's standard metrics for model assessment, Discrete Optimized Protein Energy (DOPE) [83] to choose the best three models for further analysis. However, as these scores are not reliable enough for membrane proteins (they are primarily based on the model's free energy and spacial occupation directed to water-soluble proteins) we took additional metrics into account. In particular, we used Protein Structure Analysis (ProSA) web service [64] and the online Protein Quality (ProQ) prediction server [84]. The z-score, provided by ProSA was only used for error recognition, as it indicates overall model quality with respect to an energy distribution derived from random conformations for globular proteins [64]. On the other hand, ProQ provides the LGscore [85] and MaxSub [86], based on a neural network, which were set as base for the more detailed evaluation of the models. Additionally, ProQ allows to include secondary structure information calculated with PSIPRED [37], which improves the prediction accuracy and increasing the model quality up to 15%. The ProQ analysis was only carried out, if z-scores around 2-4 were achieved using the ProQ protocol. Finally, the Ballesteros and Weinstein numbering system for class A GPCRs was applied in order to simply comparison between different receptors and complex systems [42].

Peer-reviewed version available at Molecules 2019, 24, 1196; doi:10.3390/molecules24071196

4.2. Molecular dynamics

4.2.1. System setup

Before setting up the system, the selected DR models were subjected to the Orientations of Proteins in Membranes (OPM) web-server [87–90] to calculate spatial orientations respecting to the Membrane Normal defined by the z-axis. In addition, the state of titratable residues was calculated by Propka 3.1 [91,92] within the PDB2PQR web-server [93] at a pH of 7.0. The prepared receptor structures were inserted into a rectangular box simulation with dimensions of 114 x 114 x 107 Å. The box was previously constructed with a lipid bilayer of POPC: Cholesterol (9:1) and explicitly represented water and subjected to an initial equilibration of 10 ns. Insertion of the receptors in the membrane was performed with *g_membed* package of GROMACS [94]. Sodium and chloride ions were added to neutralize the system until it reached a total concentration of 0.15 M. The final systems included approximately 370 POPC, 40 cholesterols, 125 sodium ions, 139 chloride ions and 28500 water molecules, with small variations from receptor to receptor.

4.2.2. Molecular Dynamics simulation protocol

CHARMM36 force field was used for ions, water (TIP3P model), lipids and protein parameters [95]. Prior to MD simulation, the systems were relaxed to remove any possible steric clashes by a set of 50000 steps of Steepest Descent energy minimization. Equilibration was performed afterwards as following: the system was heated using Nosé-Hoover thermostat from 0 to 310.15 K in the NVT ensemble over 100 ps with harmonic restraints of 10.0 kcal/mol. Then systems were subjected through a first step of NPT ensemble of 1 ns with semi isotropic pressure coupling and a pressure of one bar. Further equilibration was performed with sequential release of membrane lipids and protein's atoms with a final step of NPT ensemble with harmonic restraints on the protein of 1.0 kcal/mol, for a total of 5 ns of restrained equilibration.

MD simulations of all DR models were performed with the periodic boundary condition to produce isothermical-isobaric ensembles using GROMACS 5.1.1 [94]. The Particle Mesh Ewald (PME) method [96] was used to calculate the full electrostatic energy of a unit cell in a macroscopic lattice of repeating images. Temperature was regulated using the Nosé-Hoover thermostat at 310.15 K. Pressure was regulated using the Parrinello-Rahman algorithm. The equations of motion were integrated using leapfrog algorithm with a time step of 2 fs. All bonds, involving hydrogen atoms within protein and lipid molecules were constrained using the LINear Constraint Solver (LINCS) algorithm [97]. Then an independent simulation of 100 ns was initialized from the final snapshot of the restrained equilibration from each DR, for a total of 5 simulations. Additionally, a cut-off distance of 12 Å was attributed for Coulombic and van der Waals interactions. Trajectory snapshots were saved every 5 ns. Trajectory analysis was performed by in-house scripting using Visual Molecular Dynamics (VMD) [98,99].

Preprints (www.preprints.org) | NOT PEER-REVIEWED | Posted: 6 February 2019 doi:10.20944/preprints201902.0064.v1

Peer-reviewed version available at Molecules 2019, 24, 1196; doi:10.3390/molecules24071196

4.3. Molecular docking

4.3.1. Ligand dataset

The following ligands were docked into the receptor decoys: Dopamine, 7-hydroxy-*N*,*N*-dipropyl-2-aminotetralin (7-OH-DPAT), apomorphine, bromocriptine, clozapine, nemonapride, sulpiride, SCH23390, SKF38393, eticlopride, risperidone, aripiprazole, haloperidole, spiperone and chlorpromazine (**Table 2**). All structures were obtained from the DrugBank database (https://www.drugbank.ca) or from ChemSpider (http://www.chemspider.com) [100].

Table 2 - Ligands used for molecular docking and information on their function.

	LIGAND	FUNCTION	BP	REFERENCES
DOPAMINE	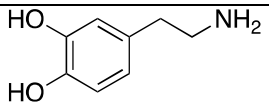	Endogenous agonist of all DR	OBP	[38,43,101]
7-OH-DPAT	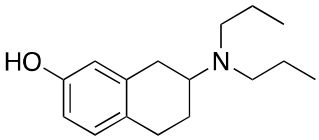	Synthetic D_3R selective agonist	OBP	[38,101,102]
APOMORPHINE	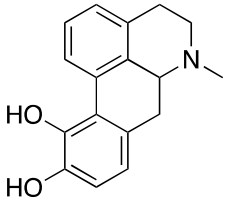	D_2R selective agonist	OBP	[38,43,101]
BROMOCRIPTINE	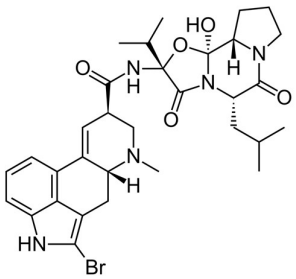	D_2R selective agonist	OBP	[38,101]
CLOZAPINE	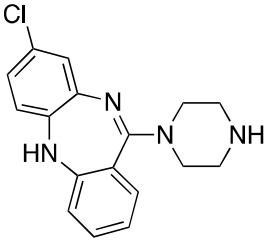	"Dirty drug", multiple receptor binding	OBP	[38,101,103,104]
NEMONAPRIDE	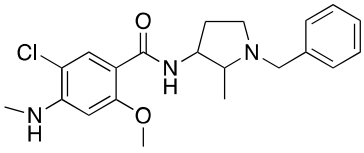	D_2R/D_3R selective antagonist	OBP+SBP	[28,38,46,101]

Preprints (www.preprints.org) | NOT PEER-REVIEWED | Posted: 6 February 2019 doi:10.20944/preprints201902.0064.v1

Peer-reviewed version available at *Molecules* **2019**, *24*, 1196; doi:10.3390/molecules24071196

SULPIRIDE	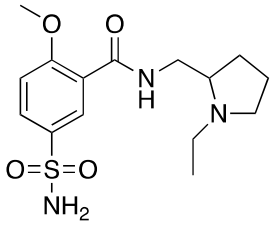	"Dirty drug", multiple receptor binding	OBP+SBP	[38,101,102]
SCH23390	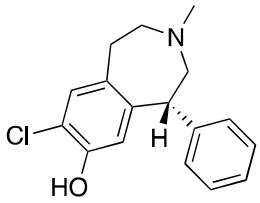	D_1R antagonist	OBP	[22,38,101,105]
SKF38393	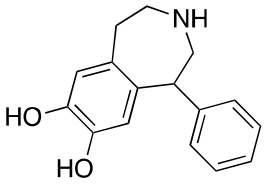	D_1R selective agonist	OBP	[22,38,101,106]
ETICLOPRIDE	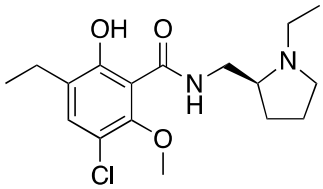	D_2R/D_3R selective antagonist	OBP+SBP	[27,102]
RISPERIDONE	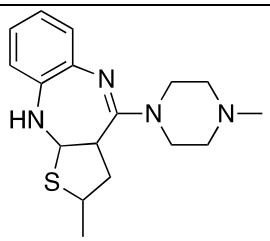	"Dirty drug", multiple receptor binding	OBP+SBP	[29,38]
ARIPIPRAZOLE	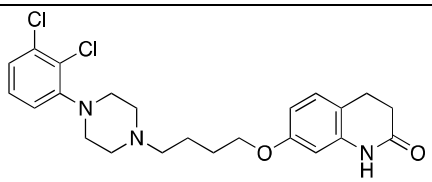	Partial D_2R agonist, D_2R/D_3R heterodimer antagonist	OBP+SBP	[17,102]
HALOPERIDOLE	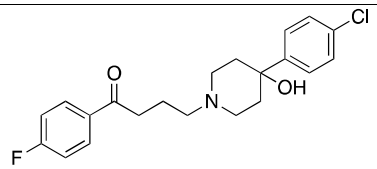	D_2R selective antagonist, D_4R antagonist	OBP+SBP	[9,38,101,103,107]
SPIPERONE	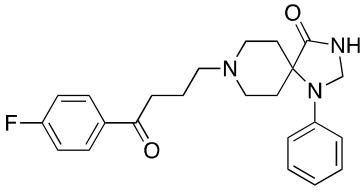	Affinity for all DR	OBP+SBP	[38,101,102]

CHLORPROMAZINE	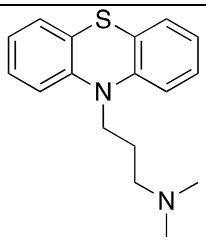	Antagonist on all DR	OBP	[38,101,108]

Abbreviations: DR-dopamine receptors, BP-binding pocket, OBP-orthosteric binding pocket, SBP-secondary binding pocket.

4.3.2. Docking procedure

DR binding pocket was defined in several experimental and computational studies [2,38,43,46,48,50,60]. Here, we used the comprehensive review by Floresca and Schetz [38] as a base for exploration of the DR binding pocket, since it contains detailed experimental data. A summary of the procedure can be better reviewed in Bueschbell *et al.* [41]. AutoDock4.2 (version AutoDock 4.2.6, released in 2009) was used to perform ligand docking [109]. DR hydrogens were added and Kollman united atom charges were assigned. Hydrogens were also added to the ligand and Gasteiger-Marsili was used to calculate charges. Before docking an energy, grid was created using AutoGrid (version AutoGrid 4.2.6, released 2009) with a box-size varying with the times step and ligand. For each docking simulation 100 independent Lamarckian genetic algorithm (LGA) runs were performed with the number of energy evaluations set to 10.000.000, the population size set to 200 and the maximum number of generations set to 27.000. Default settings were maintained for the rest of the parameters. Docked conformations within a RMSD of 2 Å were clustered. The most populated and lowest energy cluster (Gibbs free energy of binding) was used for conformational analysis. To find the local energy minimum of the binding site with a limited search space to that region, a low-frequency local search method was used. The 100 conformations obtained from docking were clustered by low-energy and RMSD. The top-ranked conformations within the best 3 clusters were visually inspected. The docking parameters were not changed for any ligand, only the residues treated as flexible in the docking protocol differed between the ligands. The flexible residues for each DR model are summarized in **Table 3**.

Table 3 - Flexible residues used in the molecular docking different ligands

LIGAND	FLEXIBLE RESIDUES IN B&W NUMBERING
DOPAMINE	3.32Asp, 5.42Ser, 5.43Ser, 5.46Ser, 6.48Trp, 6.51Phe, 6.52Phe, 6.55His/Asn
7-OH-DPAT	
APOMORPHINE	3.32Asp, 3.36/3.35Cys, 5.42Ser, 5.43Ser, 5.46Ser, 6.48Trp, 6.51Phe, 6.52Phe, 6.55His/Asn
BROMOCRIPTINE	
CLOZAPINE	3.32Asp, 3.33Val, 3.36Cys, 5.42Ser, 5.43Ser, 5.46Ser, 6.48Trp, 6.55His/Asn
NEMONAPRIDE	2.57Val, 3.32Asp, 5.42Ser, 5.43Ser, 5.46Ser, 6.48Trp, 6.51Phe, 6.52Phe, 7.43Tyr
SULPIRIDE	3.32Asp, 6.48Trp, 5.42Ser, 5.43Ser, 5.46Ser, 6.55His/Asn, 7.43Tyr, 6.51Phe
SCH23390	3.32Asp, 6.48Trp, 5.42Ser, 5.43Ser, 5.46Ser, 6.55His/Asn, 6.51Phe, 6.52Phe

Preprints (www.preprints.org) | NOT PEER-REVIEWED | Posted: 6 February 2019 doi:10.20944/preprints201902.0064.v1

Peer-reviewed version available at Molecules 2019, 24, 1196; doi:10.3390/molecules24071196

SKF38393	
ETICLOPRIDE	3.32Asp, 6.48Trp, 5.42Ser, 5.43Ser, 5.46Ser, 6.55His/Asn, 7.43Tyr, 6.51Phe, 6.52Phe
RISPERIDONE	3.32Asp, 6.48Trp, 3.36Cys, 6.55His/Asn, 2.57Val, 5.42Ser, 5.43Ser, 5.46Ser
ARIPIPRAZOLE	3.32Asp, 6.48Trp, 3.33Val, 5.42Ser, 5.43Ser, 5.46Ser, 7.43Tyr, 6.55His/Asn
HALOPERIDOLE	3.32Asp, 6.48Trp, 6.51Phe, 6.52Phe, 3.36Cys, 2.57Val, 5.42Ser, 5.43Ser, 5.46Ser
SPIPERONE	3.32Asp, 6.48Trp, 5.42Ser, 5.43Ser, 5.46Ser, 3.36Cys, 6.55His/Asn, 2.57Val
CHLORPROMAZINE	3.32Asp, 6.48Trp, 5.42Ser, 5.43Ser, 5.46Ser, 6.55His/Asn, 3.36Cys, 6.51Phe

4.3.3. Analysis of molecular docking

In this study, 15 DR ligands were docked to the homology model and to different conformational arrangements retrieved at every 5 ns for the 55-100 ns range for each DR simulation (825 dockings in total). All distances between the center of mass of the ligand and the alpha-C-atom (Cα) of the residues, treated as flexible in the docking protocol, were calculated using in-house PyMOL scripts[2,10,38,43,48,50] as well as previously published work [41]. We also develop in-house BINANA scripts to predict the main receptor-ligand interactions [30]. BINANA is an open-source python-implemented algorithm which uses output files from AutoDock [109] for the analysis of interactions and visualizes them in the free molecular-visualization program VMD [98]. Key binding characteristics such as hydrogen bonds, hydrophobic contacts, salt-bridges and π-interactions were calculated with BINANA.

Supplementary Materials

Figure S1 – RMSD throughout the 100 ns of simulation for all DR models; Figure S2 – Important residues for molecular docking of Dopamine to the DR models; Figure S3 – Redocking of ligands with their respective DR and bound ligand; Figure S4 - Molecular docking of Dopamine at the D1R – D5R during 0 – 60 ns; Figure S5 - Molecular docking of Dopamine at the D1R – D5R during 65 – 75 ns; Figure S6 - Molecular docking of Dopamine at the D1R – D5R during 80 – 90 ns; Figure S7 - Molecular docking of Dopamine at the D1R – D5R during 95 and 100 ns; Figure S8 - Results of the molecular docking of bromocriptine, clozapine, sulpiride, eticlopride, risperidone, aripiprazole and risperidone for all DR subtypes at time points [ns]; Figure S9 – Total interactions counted for each DR over time points [ns]; Figure S10 - Pair-wise prediction results for dopamine; Figure S11 - Pair-wise prediction results for 7-OH-DPAT; Figure S12 – Pair-wise prediction results for apomorphine; Figure S13 – Pair-wise prediction results for bromocriptine; Figure S14 - Pair-wise prediction results for clozapine; Figure S15 – Pair-wise prediction results for nemonapride; Figure S16 – Pair-wise prediction results for sulpiride; Figure S17 – Pari-wise prediction results for SCH23390; Figure S18 – Pair-wise prediction results for SKF38393; Figure S19 – Pair-wise prediction results for eticlopride; Figure S20 – Pair-wise prediction results for risperidone; Figure S21 – Pair-wise prediction results for aripiprazole; Figure S22 – Pair-wise prediction results for haloperidole; Figure S23 – Pair-wise prediction results for spiperone; Figure S24 –

Pair-wise prediction results for chlorpromazine. Table S1 - Comparison between the total and transmembrane specific identity [%] of the DR model with their crystal structure templates calculated with Clustal Omega; Table S2 - Summary of the structures used in literature for defining the binding pocket for the D_2R and source (experimental and computational); Table S3 - Docking results for the D_1R; Table S4 - Docking results for the D_2R; Table S5 -Docking results for the D_3R; Table S6 - Docking results for the D_4R; Table S7 - Docking results for the D_5R; Table S8 - Docking results for the crystal structure templates of D_2R (6CM4), D_3R (3PBL) and D_4R (5WIU) docked with their co-crystalized ligands; Table S9 - D_1R residues with Ballesteros & Weinstein-numbering participating in different interaction types sorted by ligands; Table S10 - D_2R residues with Ballesteros & Weinstein-numbering participating in different interaction types sorted by ligands; Table S11 - D_3R residues with Ballesteros & Weinstein-numbering participating in different interaction types sorted by ligands; Table S12 - D_4R residues with Ballesteros & Weinstein-numbering participating in different interaction types sorted by ligands; Table S13 - D_5R residues with Ballesteros & Weinstein-numbering participating in different interaction types sorted by ligands.

Acknowledgments

This work was carried out with funding from BIGs Drugs Graduate school. Irina S. Moreira acknowledges support by the Fundação para a Ciência e a Tecnologia (FCT) Investigator programme - IF/00578/2014 (co-financed by European Social Fund and Programa Operacional Potencial Humano). This work was also financed by the European Regional Development Fund (ERDF), through the Centro 2020 Regional Operational Programme under project CENTRO-01-0145-FEDER-000008: BrainHealth 2020. We also acknowledge the grant PTDC/QUI-OUT/32243/2017 financed by national funds through the FCT / MCTES and/or State Budget.

Author Contributions

B. B., A.J.P. and C.A.V.B. performed the experiments; B.B, A.J.P. and C.A.V.B. analyzed the data; B.B., A.C.S and I.S.M conceived and designed the experiments; all authors wrote the paper.

Conflicts of Interest: The authors declare no conflict of interest.

References

[1] Beaulieu, J.-M.; Gainetdinov, R. R. The Physiology, Signaling, and Pharmacology of Dopamine Receptors. *Pharmacol. Rev.* **2011**, *63* (1), 182–217.

[2] Platania, C. B. M.; Salomone, S.; Leggio, G. M.; Drago, F.; Bucolo, C. Homology Modeling of Dopamine D 2 and D 3 Receptors : Molecular Dynamics Refinement and Docking Evaluation. *PLoS One* **2012**, *7* (9).

[3] Jaber, M.; Robinson, S. W.; Missale, C.; Caron, M. G. Dopamine receptors and brain function.

Neuropharmacology **1997**, *35* (11), 1503–1519.

[4] Seeman, P. Atypical Antipsychotics: Mechanism of Action. **2002**, *47* (1), 27–38.

[5] Rangel-Barajas, C.; Coronel, I.; Florán, B. Dopamine Receptors and Neurodegeneration. *Aging Dis.* **2015**, *6* (5), 349.

[6] Leggio, G. M.; Bucolo, C.; Platania, C. B. M.; Salomone, S.; Drago, F. Current drug treatments targeting dopamine D3 receptor. *Pharmacol. Ther.* **2016**, *165*, 164–177.

[7] Rosenbaum, D. M.; Rasmussen, S. G. F.; Kobilka, B. K. The structure and function of G protein-coupled receptors. *Nature* **2009**, *459* (7245), 356–363.

[8] Maurice, P.; Guillaume, J. L.; Benleulmi-Chaachoua, A.; Daulat, A. M.; Kamal, M.; Jockers, R. GPCR-Interacting Proteins, Major Players of GPCR Function. *GPCR-Interacting Proteins, Major Players of GPCR Function*, 1st ed.; Elsevier Inc., 2011; Vol. 62.

[9] Madras, B. K. History of the discovery of the antipsychotic dopamine D2 receptor: A basis for the dopamine hypothesis of schizophrenia. *J. Hist. Neurosci.* **2013**, *22* (1), 62–78.

[10] Ekhteiari Salmas, R.; Serhat Is, Y.; Durdagi, S.; Stein, M.; Yurtsever, M. A QM protein–ligand investigation of antipsychotic drugs with the dopamine D2 Receptor (D2R). *J. Biomol. Struct. Dyn.* **2017**, No. August, 1–10.

[11] Sykes, D. A.; Moore, H.; Stott, L.; Holliday, N.; Javitch, J. A.; Lane, J. R.; Charlton, S. J. Extrapyramidal side effects of antipsychotics are linked to their association kinetics at dopamine D2 receptors. *Nat. Commun.* **2017**, *8* (1), 763.

[12] Banala, A. K.; Levy, B. A.; Khatri, S. S.; Furman, C. A.; Roof, R. A.; Mishra, Y.; Gri, S. A.; Sibley, D. R.; Luedtke, R. R.; Newman, A. H. N-(3-Fluoro-4-(4-(2-methoxy or 2,3-dichlorophenyl)piperazine-1-yl)arylcarboxamides as selective dopamine D3 receptor ligands: critical role of the carboxamide linker for D3 recetpor selectivity. *J. Med. Chem.* **2011**, *54*, 3581–3594.

[13] Newman, A. H.; Beuming, T.; Banala, A. K.; Donthamsetti, P.; Pongetti, K.; LaBounty, A.; Levy, B. A.; Cao, J.; Michino, M.; Luedtke, R. R.; Javitch, J. A.; Shi, L. Molecular determinants of selectivity and efficacy at the dopamine D3 receptor. *J. Med. Chem.* **2012**, *55* (15), 6689–6699.

[14] Damsma, G.; Bottema, T.; Westerink, B. H. C.; Tepper, P. G.; Dijkstra, D.; Pugsley, T. A.; MacKenzie, R. G.; Heffner, T. G.; Wikström, H. Pharmacological aspects of R-(+)-7-OH-DPAT, a putative dopamine D3 receptor ligand. *Eur. J. Pharmacol.* **1993**, *249*, 9–10.

[15] Lévesque, D.; Diaz, J.; Pilon, C.; Martres, M. P.; Giros, B.; Souil, E.; Schott, D.; Morgat, J. L.; Schwartz, J. C.; Sokoloff, P. Identification, characterization, and localization of the dopamine D3 receptor in rat brain using 7-[3H]hydroxy-N,N-di-n-propyl-2-aminotetralin. *Proc. Natl. Acad. Sci. U. S. A.* **1992**, *89* (17), 8155–8159.

[16] Sampson, D.; Zhu, X. Y.; Eyunni, S. V. K.; Etukala, J. R.; Ofori, E.; Bricker, B.; Lamango, N. S.; Setola, V.; Roth, B. L.; Ablordeppey, S. Y. Identification of a new selective dopamine D4receptor ligand. *Bioorganic Med. Chem.* **2014**, *22* (12), 3105–3114.

[17] Burris, K. D.; Molski, T. F.; Xu, C.; Ryan, E.; Tottori, K.; Kikuchi, T.; Yocca, F. D.; Molinoff, P. B. Aripiprazole, a novel antipsychotic, is a high-affinity partial agonist at human dopamine D2 receptors. *J. Pharmacol. Exp. Ther.* **2002**, *302* (1), 381–389.

[18] Zhang, J.; Xiong, B.; Zhen, X.; Zhang, A. Dopamine D1 receptor ligands: Where are we now and where are we going. *Med. Res. Rev.* **2009**, *29* (2), 272–294.

[19] Conroy, J. L.; Free, R. B.; Sibley, D. R. Identification of G Protein-Biased Agonists That Fail to Recruit β-Arrestin or Promote Internalization of the D1 Dopamine Receptor. *ACS Chem. Neurosci.* **2015**, *6* (4), 681–692.

[20] Butini, S.; Nikolic, K.; Kassel, S.; Brückmann, H.; Filipic, S.; Agbaba, D.; Gemma, S.; Brogi, S.; Brindisi, M.; Campiani, G.; Stark, H. Polypharmacology of dopamine receptor ligands. *Prog. Neurobiol.* **2016**, *142*, 68–103.

[21] Lee, S. M.; Kant, A.; Blake, D.; Murthy, V.; Boyd, K.; Wyrick, S. J.; Mailman, R. B. SKF-83959 is not a highly-biased functionally selective D1dopamine receptor ligand with activity at phospholipase C. *Neuropharmacology* **2014**, *86*, 145–154.

[22] Arimitsu, E.; Ogasawara, T.; Takeda, H.; Sawasaki, T.; Ikeda, Y.; Hiasa, Y.; Maeyama, K. The ligand binding ability of dopamine D<inf>1</inf> receptors synthesized using a wheat germ cell-free protein synthesis system with liposomes. *Eur. J. Pharmacol.* **2014**, *745*, 117–122.

[23] Giorgioni, G.; Piergentili, a; Ruggieri, S.; Quaglia, W. Dopamine D5 receptors: a challenge to medicinal chemists. *Mini Rev. Med. Chem.* **2008**, *8* (10), 976–995.

[24] Sliwoski, G.; Kothiwale, S.; Meiler, J.; Lowe, E. W. Computational methods in drug discovery. *Comput. Methods Drug Discov.* **2014**, *66* (1), 334–395.

[25] Jain, A. Computer Aided Drug Design & QSAR. *J. Phys. Conf. Ser.* **2017**, *884* (1), 012072.

[26] Shin, W. H.; Christoffer, C. W.; Kihara, D. In silico structure-based approaches to discover protein-protein interaction-targeting drugs. *Methods* **2017**, 1–11.

[27] Chien, E. Y. T.; Liu, W.; Zhao, Q.; Katritch, V.; Han, G. W.; Michael, a; Shi, L.; Newman, A. H.; Javitch, J. a; Cherezov, V.; Stevens, R. C. Structure of the human dopamine D3 receptor in complex with a D2/D3 selective antagonist. *Science (80-.).* **2011**, *330* (6007), 1091–1095.

[28] Wang, S.; Wacker, D.; Levit, A.; Che, T.; Betz, R. M.; Mccorvy, J. D.; Venkatakrishnan, A. J.; Huang, X.-P.; Dror, R. O.; Shoichet, B. K.; Roth, B. L. D4 dopamine receptor high-resolution structures enable the discovery of selective agonists. **2017**, *386* (6361), 381–386.

[29] Wang, S.; Che, T.; Levit, A.; Shoichet, B. K.; Wacker, D.; Roth, B. L. Structure of the D2 dopamine receptor bound to the atypical antipsychotic drug risperidone. *Nat. 2018* **2018**, 1–24.

[30] Durrant, J. D.; McCammon, J. A. BINANA: A novel algorithm for ligand-binding characterization. *J. Mol. Graph. Model.* **2011**, *29* (6), 888–893.

[31] Webb, B.; Sali, A.; Francisco, S. Comparative Protein Structure Modeling Using MODELLER. *Curr Protoc Bioinforma.* **2017**, *54* (ii), 1–55.

[32] Chien, E. Y. T.; Liu, W.; Zhao, Q.; Katritch, V.; Won Han, G.; Hanson, M. A.; Shi, L.; Newman, A. H.; Javitch, J. A.; Cherezov, V.; Stevens, R. C. Structure of the Human Dopamine D3 Receptor in Complex with a D2/D3 Selective Antagonist. *Science (80-.).* **2010**, *330* (6007), 1091–1095.

[33] Berman, H. M.; Westbrook, J.; Feng, Z.; Gilliland, G.; Bhat, T. N.; Weissig, H.; Shindyalov, I. N.; Bourne, P. E. The protein data bank. *Nucleic Acids Res.* **2000**, *28* (1), 235–242.

[34] Altschul, S. F.; Gish, W.; Miller, W.; Myers, E. W.; Lipman, D. J. Basic local alignment search tool. *J. Mol. Biol.* **1990**, *215* (3), 403–410.

[35] Sievers, F.; Wilm, A.; Dineen, D.; Gibson, T. J.; Karplus, K.; Li, W.; Lopez, R.; McWilliam, H.; Remmert, M.; Söding, J.; Thompson, J. D.; Higgins, D. G. Fast, scalable generation of high-quality protein multiple sequence alignments using Clustal Omega. *Mol. Syst. Biol.* **2011**, *7* (539).

[36] Shen, M.; Sali, A. Statistical potential for assessment and prediction of protein structures. *Protein Sci.* **2006**, *15* (11), 2507–2524.

[37] McGuffin, L. J.; Bryson, K.; Jones, D. T. The PSIPRED protein structure prediction server. *Bioinformatics* **2000**, *16* (4), 404–405.

[38] Floresca, C. Z.; Schetz, J. A. Dopamine Receptor Microdomains Involved in Molecular Recognition and the Regulation of Drug Affinity and Function. *J. Recept. Signal Transduct.* **2004**, *24* (3), 207–239.

[39] Cummings, D. F.; Ericksen, S. S.; Goetz, A.; Schetz, J. A. Transmembrane Segment Five Serines of the D4 Dopamine Receptor Uniquely Influence the Interactions of Dopamine, Norepinephrine, and Ro10-4548. *J. Pharmacol. Exp. Ther.* **2010**, *333* (3), 682–695.

[40] Ericksen, S. S.; Cummings, D. F.; Teer, M. E.; Amdani, S.; Schetz, J. A. Ring Substituents on Substituted Benzamide Ligands Indirectly Mediate Interactions with Position 7.39 of Transmembrane Helix 7 of the D4 Dopamine Receptor. *J. Pharmacol. Exp. Ther.* **2012**, *342* (2), 472–485.

[41] Bueschbell, B.; Preto, A. J.; Barreto, C. A. V.; Schiedel, A. C.; Moreira, I. S. Creating a valid in silico Dopamine D2-receptor model for small molecular docking studies. In *MOL2NET, International Conference Series on Multidisciplinary Sciences*; 2017; Vol. 3, pp 1–6.

[42] Ballesteros, J. A.; Weinstein, H. Integrated methods for the construction of three dimensional models and computational probing of structure-function relations in G-protein coupled receptors. *Methods Neurosci.* **1995**, *25*, 366–428.

[43] Salmas, R. E.; Yurtsever, M.; Stein, M.; Durdagi, S. Modeling and protein engineering studies of active and inactive states of human dopamine D2 receptor (D2R) and investigation of drug/receptor interactions. *Mol. Divers.* **2015**, *19* (2), 321–332.

[44] Moreira, I. S.; Shi, L.; Freyberg, Z.; Ericksen, S. S.; Weinstein, H.; Javitch, J. A. Structural Basis of Dopamine Receptor Activation. In *The Dopamine Receptors*; Neve, K. A., Ed.; Humana/Springer, 2010; pp 47–73.

[45] Huang, E. S. Construction of a sequence motif characteristic of aminergic G protein-coupled receptors. *Protein Sci.* **2003**, *12* (7), 1360–1367.

[46] Tschammer, N.; Dörfler, M.; Hübner, H.; Gmeiner, P. Engineering a GPCR-ligand pair that simulates the activation of D 2L by dopamine. *ACS Chem. Neurosci.* **2010**, *1* (1), 25–35.

[47] Kling, R. C.; Tschammer, N.; Lanig, H.; Clark, T.; Gmeiner, P. Active-state model of a dopamine D2 receptor - Galpha-i complex stabilized by aripiprazole-type partial agonists. *PLoS One* **2014**, *9* (6), 1–10.

[48] Kalani, M. Y. S.; Vaidehi, N.; Hall, S. E.; Trabanino, R. J.; Freddolino, P. L.; Kalani, M. a; Floriano, W. B.; Kam, V. W. T.; Goddard, W. a. The predicted 3D structure of the human D2 dopamine receptor and the binding site and binding affinities for agonists and antagonists. *Proc. Natl. Acad. Sci.* **2004**, *101* (11), 3815–3820.

[49] Holst, B.; Nygaard, R.; Valentin-Hansen, L.; Bach, A.; Engelstoft, M. S.; Petersen, P. S.; Frimurer, T. M.; Schwartz, T. W. A conserved aromatic lock for the tryptophan rotameric switch in TM-VI of seven-transmembrane receptors. *J. Biol. Chem.* **2010**, *285* (6), 3973–3985.

[50] Männel, B.; Jaiteh, M.; Zeifman, A.; Randakova, A.; Möller, D.; Hübner, H.; Gmeiner, P.; Carlsson, J. Structure-guided screening for functionally selective D2 dopamine receptor ligands from a virtual chemical library. *ACS Chem. Biol.* **2017**, acschembio.7b00493.

[51] Wang, S.; Wacker, D.; Levit, A.; Che, T.; Betz, R. M.; Mccorvy, J. D.; Venkatakrishnan, A. J.; Huang, X.-

P.; Dror, R. O.; Shoichet, B. K.; Roth, B. L. D 4 dopamine receptor high-resolution structures enable the discovery of selective agonists. **2017**.

[52] Durdagi, S.; Salmas, R. E.; Stein, M.; Yurtsever, M.; Seeman, P. Binding Interactions of Dopamine and Apomorphine in D2High and D2Low States of Human Dopamine D2 Receptor Using Computational and Experimental Techniques. *ACS Chem. Neurosci.* **2016**, *7* (2), 185–195.

[53] Boyd, K. N.; Mailman, R. B. Dopamine receptor signaling and cirrent and future antipyschotic drugs. *Handb Exp Pharmacol* **2012**, *212* (212), 53–86.

[54] Bergman, J.; Madras, B. K.; Spealman, R. D. Behavioral effects of D1 and D2 dopamine receptor antagonists in squirrel monkeys. *J.Pharmacol.Exp.Ther.* **1991**, *258* (d), 910–917.

[55] Chen, T.; Hu, Y.; Lin, X.; Huang, X.; Liu, B.; Leung, P.; Chan, S. O.; Guo, D.; Jin, G. Dopamine signaling regulates the projection patterns in the mouse chiasm. *Brain Res.* **2015**, *1625*, 324–336.

[56] Hidaka, K.; Matsumoto, M.; Tada, S.; Tasaki, Y.; Yamaguchi, T. Differential effects of [3H]nemonapride and [3H]spiperone binding on human dopamine D4 receptors. *Neurosci. Lett.* **1995**, *186*, 145–148.

[57] Bosch, E.; Barnes, C. L.; Brennan, N. L.; Eakins, G. L.; Breyfogle, B. E. Cation-Induced π-stacking. *J. Org. Chem.* **2008**, *73*, 3931–3934.

[58] Frontera, A.; Quiñonero, D.; Deyà, P. M. Cation-π and anion-π interactions. *Wiley Interdiscip. Rev. Comput. Mol. Sci.* **2011**, *1* (3), 440–459.

[59] Davis, A. M.; Teague, S. J. Hydrogen bonding, hydrophobic interactions, and failure of the rigid receptor hypothesis. *Angew. Chemie - Int. Ed.* **1999**, *38*, 736–749.

[60] Sukalovic, V.; Soskic, V.; Sencanski, M.; Andric, D.; Kostic-Rajacic, S. Determination of key receptor-ligand interactions of dopaminergic arylpiperazines and the dopamine D2 receptor homology model. *J. Mol. Model.* **2013**, *19* (4), 1751–1762.

[61] Moreira, I. S. Structural features of the G-protein/GPCR interactions. *Biochim. Biophys. Acta - Gen. Subj.* **2014**, *1840* (1), 16–33.

[62] Halgren, T. A.; Murphy, R. B.; Friesner, R. A.; Hege, S. B.; Klicic, J. J.; Mainz, D. T.; Repasky, M. P.; Knoll, E. H.; Shelley, M.; Perry, J. K.; Shaw, D. E.; Francis, P.; Shenkin, P. S. Glide: A New Approach for Rapid, Accurate Docking and Scoring. 1. Method and Assessment of Docking Accuracy. *J. Med. Chem.* **2004**, *47* (7), 1739–1749.

[63] Hou, J.; Charron, C. L.; Fowkes, M. M.; Luyt, L. G. Bridging computational modeling with amino-acid replacements to investigate GHS-R1a-peptidomimetic recognition. *Eur. J. Med. Chem.* **2016**, *123*, 822–833.

[64] Wiederstein, M.; Sippl, M. J. ProSA-web: Interactive web service for the recognition of errors in three-dimensional structures of proteins. *Nucleic Acids Res.* **2007**, *35* (Web Server issue), 407–410.

[65] Wallner, B.; Elofsson, A. Can correct protein models be identified? *Protein Sci.* **2003**, *12* (5), 1073–1086.

[66] Gaete-Eastman, C.; Morales-Quintana, L.; Herrera, R.; Moya-León, M. A. In-silico analysis of the structure and binding site features of an α-expansin protein from mountain papaya fruit (VpEXPA2), through molecular modeling, docking, and dynamics simulation studies. *J. Mol. Model.* **2015**, *21* (5), 1–12.

[67] Valizade Hasanloei, M. A.; Sheikhpour, R.; Sarram, M. A.; Sheikhpour, E.; Sharifi, H. A combined Fisher and Laplacian score for feature selection in QSAR based drug design using compounds with known and unknown activities. *J. Comput. Aided. Mol. Des.* **2018**, *32* (2), 375–384.

[68] Kumar, S. P. PLHINT: A knowledge-driven computational approach based on the intermolecular H bond interactions at the protein-ligand interface from docking solutions. *J. Mol. Graph. Model.* **2018**, *79*, 194–212.

[69] Trisciuzzi, D.; Nicolotti, O.; Miteva, M. A.; Villoutreix, B. O. Analysis of solvent-exposed and buried co-crystallized ligands: a case study to support the design of novel protein–protein interaction inhibitors. *Drug Discov. Today* **2018**.

[70] Tanina, A.; Wohlkönig, A.; Soror, S. H.; Flipo, M.; Villemagne, B.; Prevet, H.; Déprez, B.; Moune, M.; Perée, H.; Meyer, F.; Baulard, A. R.; Willand, N.; Wintjens, R. A comprehensive analysis of the protein-ligand interactions in crystal structures of Mycobacterium tuberculosis EthR. *Biochim. Biophys. Acta - Proteins Proteomics* **2018**, #pagerange#.

[71] Salmas, R. E.; Yurtsever, M.; Durdagi, S. Atomistic molecular dynamics simulations of typical and atypical antipsychotic drugs at the dopamine D2 receptor (D2R) elucidates their inhibition mechanism. *J. Biomol. Struct. Dyn.* **2016**, *35* (4), 1–17.

[72] Schetz, J. A.; Kim, O.-J.; Sibley, D. R. Pharmacological Characterization of Mammalian D 1 and D 2 Dopamine Receptors Expressed in Drosophila Schneider-2 Cells. *J. Recept. Signal Transduct.* **2003**, *23* (1), 99–109.

[73] Bourne, J. A. SCH23390: The First Selective Dopamine D1-Like Receptor Antagonist. *CNS Drug Rev.* **2006**, *7* (4), 399–414.

[74] Ferreira De Freitas, R.; Schapira, M. A systematic analysis of atomic protein-ligand interactions in the PDB. *Medchemcomm* **2017**, *8* (10), 1970–1981.

[75] Hugo, E. A.; Cassels, B. K.; Fierro, A. Functional roles of T3.37 and S5.46 in the activation mechanism of the dopamine D1 receptor. *J. Mol. Model.* **2017**, *23* (4).

[76] Wang, Q.; MacH, R. H.; Luedtke, R. R.; Reichert, D. E. Subtype selectivity of dopamine receptor ligands: Insights from structure and ligand-based methods. *J. Chem. Inf. Model.* **2010**, *50* (11), 1970–1985.

[77] Simpson, M. M.; Ballesteros, J. A.; Chiappa, V.; Chen, J.; Suehiro, M.; Hartman, D. S.; Godel, T.; Snyder, L. A.; Sakmar, T. P.; Javitch, J. A. Dopamine D4/D2 receptor selectivity is determined by A divergent aromatic microdomain contained within the second, third, and seventh membrane-spanning segments. *Mol. Pharmacol.* **1999**, *56* (6), 1116–1126.

[78] Zarrindast, M. R.; Honardar, Z.; Sanea, F.; Owji, A. A. SKF 38393 and SCH 23390 inhibit reuptake of serotonin by rat hypothalamic synaptosomes. *Pharmacology* **2011**, *87* (1–2), 85–89.

[79] Pettersson, I.; Gundertofte, K.; Palm, J.; Liljefors, T. A Study on the Contribution of the 1-Phenyl Substituent to the Molecular Electrostatic Potentials of Some Benzazepines in Relation to Selective Dopamine D-1 Receptor Activity. *J. Med. Chem.* **1992**, *35* (3), 502–507.

[80] Ekhteiari Salmas, R.; Serhat Is, Y.; Durdagi, S.; Stein, M.; Yurtsever, M. A QM protein–ligand investigation of antipsychotic drugs with the dopamine D2 Receptor (D2R). *J. Biomol. Struct. Dyn.* **2017**, *1102* (November), 1–10.

[81] Scarselli, M.; Novi, F.; Schallmach, E.; Lin, R.; Baragli, A.; Colzi, A.; Griffon, N.; Corsini, G. U.; Sokoloff, P.; Levenson, R.; Vogel, Z.; Maggio, R. D2/D3 Dopamine Receptor Heterodimers Exhibit Unique Functional Properties. *J. Biol. Chem.* **2001**, *276* (32), 30308–30314.

[82] Ciliax, B. J.; Nash, N.; Heilman, C.; Sunahara, R. K.; Hartney, A.; Tiberi, M.; Rye, D. B.; C, C. M.; Niznik, H. B.; Levey, A. I. Dopamine D5 receptor immunolocalization in rat and monkey brain. *Synapse* **2000**, *37*,

125–145.

[83] Shen, M.-Y.; Sali, A. Statistical potential for assessment and prediction of protein structures. *Protein Sci.* **2006**, *15*, 2507–2524.

[84] Wallner, B.; Elofsson, A. Identification of correct regions in protein models using structural, alignment, and consensus information. *Protein Sci.* **2006**, *15*, 900–913.

[85] Cristobal, S.; Zemla, a; Fischer, D.; Rychlewski, L.; Elofsson, a. A study of quality measures for protein threading models. *BMC Bioinformatics* **2001**, *2*, 5.

[86] Siew, N.; Elofsson, A.; Rychlewski, L.; Fischer, D. MaxSub: An automated measure for the assessment of protein structure prediction quality. *Bioinformatics* **2000**, *16* (9), 776–785.

[87] Lomize, M. A.; Pogozheva, I. D.; Joo, H.; Mosberg, H. I.; Lomize, A. L. OPM database and PPM web server: Resources for positioning of proteins in membranes. *Nucleic Acids Res.* **2012**, *40* (D1), 370–376.

[88] Lomize, A. L.; Pogozheva, I. D.; Lomize, M. A.; Mosberg, H. I. Positioning of proteins in membranes: A computational approach - Lomize - 2009 - Protein Science - Wiley Online Library. *Protein Sci.* **2006**, *15* (6), 1318–1333.

[89] Lomize, A. L.; Pogozheva, I. D.; Lomize, M. A.; Mosberg, H. I. The role of hydrophobic interactions in positioning of peripheral proteins in membranes. *BMC Struct. Biol.* **2007**, *7*, 1–30.

[90] Lomize, A. L.; Pogozheva, I. D.; Mosber. Anisotropic solvent model of the lipid bilayer. 2. Energetics of insertion of small molecules, peptides and proteins in membranes Andrei. *J. Chem. Inf. Model.* **2011**, *51* (4), 930–946.

[91] Søndergaard, C. R.; Olsson, M. H. M.; Rostkowski, M.; Jensen, J. H. Improved Treatment of Ligands and Coupling Effects in Empirical Calculation and Rationalization of pKa Values. *J. Chem. Theory Comput.* **2011**, *7* (7), 2284–2295.

[92] Olsson, M. H. M.; Søndergaard, C. R.; Rostkowski, M.; Jensen, J. H. PROPKA3: Consistent Treatment of Internal and Surface Residues in Empirical pKa Predictions. *J. Chem. Theory Comput.* **2011**, *7* (2), 525–537.

[93] Dolinsky, T. J.; Nielsen, J. E.; McCammon, J. A.; Baker, N. A. PDB2PQR: An automated pipeline for the setup of Poisson-Boltzmann electrostatics calculations. *Nucleic Acids Res.* **2004**, *32* (WEB SERVER ISS.), 665–667.

[94] Berendsen, H. J. C.; van der Spoel, D.; van Drunen, R. GROMACS: A message-passing parallel molecular dynamics implementation. *Comput. Phys. Commun.* **1995**, *91* (1–3), 43–56.

[95] Vanommeslaeghe, K.; Hatcher, E.; Acharya, C.; Kundu, S.; Zhong, S.; Shim, J.; Darian, E.; Guvench, O.; Lopes, P.; Vorobyov, I.; Mackerell, A. D. CHARMM general force field: A force field for drug-like molecules compatible with the CHARMM all-atom additive biological force fields. *J. Comput. Chem.* **2010**, *31* (4), 671–690.

[96] Darden, T.; York, D.; Pedersen, L. Particle mesh Ewald: An N*log(N) method for Ewald sums in large systems Tom. *J. Chem. Phys.* **1993**, *98* (12), 10089.

[97] Hess, B.; Bekker, H.; Berendsen, H. J. C.; Fraaije, J. G. E. M. LINCS: a linear constraint solver for molecular simulations. *J. Comput. Chem.* **1997**, *18*, 1463–1472.

[98] Humphrey, W.; Dalke, A.; Schultern, K. VMD - Visual Molecular Dynamics. *J. Mol. Graph. Model.* **1996**, *14*, 33–38.

[99] Grant, B. J.; Rodrigues, A. P. C.; ElSawy, K. M.; McCammon, J. A.; Caves, L. S. D. Bio3d: An R package

for the comparative analysis of protein structures. *Bioinformatics* **2006**, *22* (21), 2695–2696.

[100] O'Boyle, N. M.; Banck, M.; James, C. A.; Morley, C.; Vandermeersch, T.; Hutchison, G. R. Open Babel: An Open chemical toolbox. *J. Cheminform.* **2011**, *3* (10), 1–14.

[101] Seeman, P.; Van Tol, H. H. Dopamine receptor pharmacology. *Trends Pharmacol.Sci.* **1994**, *15* (7), 264–270.

[102] Lawler, C. P.; Prioleau, C.; Lewis, M. M.; Mak, C.; Jiang, D.; Schetz, J. A.; Gonzalez, A. M.; Sibley, D. R.; Mailman, R. B. Interactions of the novel antipsychotic aripiprazole (OPC-14597) with dopamine and serotonin receptor subtypes. *Neuropsychopharmacology* **1999**, *20* (6), 612–627.

[103] Lindsley, C. W.; Hopkins, C. R. Return of D 4 Dopamine Receptor Antagonists in Drug Discovery. *J. Med. Chem.* **2017**, *60* (17), 7233–7243.

[104] Newton, C. L.; Wood, M. D.; Strange, P. G. Examining the effects of sodium ions on the binding of antagonists to dopamine D2 and D3 receptors. *PLoS One* **2016**, *11* (7), 1–11.

[105] Zhang, B.; Yang, X.; Tiberi, M. Functional importance of two conserved residues in intracellular loop 1 and transmembrane region 2 of Family A GPCRs: Insights from ligand binding and signal transduction responses of D1 and D5 dopaminergic receptor mutants. *Cell. Signal.* **2015**, *27* (10), 2014–2025.

[106] Andringa, G.; Drukarch, B.; Leysen, J. E.; Cools, A. R.; Stoof, J. C. The alleged dopamine D1receptor agonist SKF 83959 is a dopamine D1receptor antagonist in primate cells and interacts with other receptors. *Eur. J. Pharmacol.* **1999**, *364* (1), 33–41.

[107] López-Muñoz, F.; Alamo, C. The consolidation of neuroleptic therapy: Janssen, the discovery of haloperidol and its introduction into clinical practice. *Brain Res. Bull.* **2009**, *79* (2), 130–141.

[108] Abhijnhan, A.; Adams, C. E.; David, A.; Ozbilen, M. Depot fluspirilene for schizophrenia. *Cochrane Database Syst. Rev.* **2007**, No. 1.

[109] Morris, G. M.; Ruth, H.; Lindstrom, W.; Sanner, M. F.; Belew, R. K.; Goodsell, D. S.; Olson, A. J. AutoDock4 and AutoDockTools4: Automated docking with selective receptor flexibility. *J. Comput. Chem.* **2009**, *30* (16), 2785–2791.